APPENDIX A3. HIGHLIGHTED ARTICLES PUBLISHED IN 2005

Effects of Cloud Microphysics on Tropical Atmospheric Hydrologic Processes and Intraseasonal Variability

K. M. LAU, H. T. WU, Y. C. SUD, AND G. K. WALKER

Laboratory for Atmospheres, NASA Goddard Space Flight Center, Greenbelt, Maryland

ABSTRACT

The sensitivity of tropical atmospheric hydrologic processes to cloud microphysics is investigated using the NASA Goddard Earth Observing System (GEOS) general circulation model (GCM). Results show that a faster autoconversion rate leads to (a) enhanced deep convection in the climatological convective zones anchored to tropical land regions; (b) more warm rain, but less cloud over oceanic regions; and (c) an increased convective-to-stratiform rain ratio over the entire Tropics. Fewer clouds enhance longwave cooling and reduce shortwave heating in the upper troposphere, while more warm rain produces more condensation heating in the lower troposphere. This vertical differential heating destabilizes the tropical atmosphere, producing a positive feedback resulting in more rain and an enhanced atmospheric water cycle over the Tropics. The feedback is maintained via secondary circulations between convective tower and anvil regions (cold rain), and adjacent middle-to-low cloud (warm rain) regions. The lower cell is capped by horizontal divergence and maximum cloud detrainment near the freezing–melting (0°C) level, with rising motion (relative to the vertical mean) in the warm rain region connected to sinking motion in the cold rain region. The upper cell is found above the 0°C level, with induced subsidence in the warm rain and dry regions, coupled to forced ascent in the deep convection region.

It is that warm rain plays an important role in regulating the time scales of convective cycles, and in altering the tropical large-scale circulation through radiative–dynamic interactions. Reduced cloud–radiation feedback due to a faster autoconversion rate results in intermittent but more energetic eastward propagating Madden–Julian oscillations (MJOs). Conversely, a slower autoconversion rate, with increased cloud radiation produces MJOs with more realistic westward-propagating transients embedded in eastward-propagating supercloud clusters. The implications of the present results on climate change and water cycle dynamics research are discussed.

1. Introduction

Recently, there has been a growing body of evidence indicating the importance of tropical warm rain processes in the organization of tropical convection, modulation of clouds and rain types, and possibly global warming. Using 3 yr of data from the Tropical Rainfall Measuring Mission (TRMM), Short and Nakamura (2000) found that more than 20% of the total rain from the Tropics is derived from shallow convection. Johnson et al. (1999) showed that approximately 28% of the rainfall during the Tropical Ocean Global Atmosphere Couple Ocean–Atmosphere Research Experiment (TOGA COARE) may be accounted for by warm rain from midlevel *cumulus congestus*, and pointed to the importance of a midtropospheric inversion layer, formed by the melting of ice-phase precipitation falling from above, in limiting the growth of penetrative deep convection. They proposed that a basic trimodal (high, middle, and low), rather than the commonly accepted bimodal (high and low), cloud distribution as a more realistic description of the tropical cloud system. They also pointed out the importance of the cumulus congestus in determining the adjustment time scale of convective cycles. Wu (2003) inferred from theoretical calculations that about 20% of the latent heating in the Tropics would be contributed by mid- to low-level condensation processes in order to maintain the observed moist static stability profile. Innes et al. (2001) demonstrated that significant improvement in the simulation of the Madden–Julian oscillation (MJO) can be achieved by increasing vertical resolution, which helps to better resolve the melting level in convection in the

Corresponding author address: Dr. William K. M. Lau, Laboratory for Atmospheres, NASA Goddard Space Flight Center, Code 613, Greenbelt, MD 20771.
E-mail: lau@climate.gsfc.nasa.gov

JCLI3561

Meteorology
and Atmospheric
Physics
Printed in Austria

[1] Department of Earth System Science, University of California at Irvine, Irvine, CA, USA
[2] NASA/Goddard Space Flight Center, Greenbelt, MD, USA

Contrasting Indian Ocean SST variability with and without ENSO influence: A coupled atmosphere-ocean GCM study

Jin-Yi Yu[1] and **K. M. Lau**[2]

With 10 Figures

Summary

In this study, we perform experiments with a coupled atmosphere-ocean general circulation model (CGCM) to examine ENSO's influence on the interannual sea-surface temperature (SST) variability of the tropical Indian Ocean. The control experiment includes both the Indian and Pacific Oceans in the ocean model component of the CGCM (the Indo-Pacific Run). The anomaly experiment excludes ENSO's influence by including only the Indian Ocean while prescribing monthly-varying climatological SSTs for the Pacific Ocean (the Indian-Ocean Run). In the Indo-Pacific Run, an oscillatory mode of the Indian Ocean SST variability is identified by a multi-channel singular spectral analysis (MSSA). The oscillatory mode comprises two patterns that can be identified with the Indian Ocean Zonal Mode (IOZM) and a basin-wide warming/cooling mode respectively. In the model, the IOZM peaks about 3–5 months after ENSO reaches its maximum intensity. The basin mode peaks 8 months after the IOZM. The timing and associated SST patterns suggests that the IOZM is related to ENSO, and the basin-wide warming/cooling develops as a result of the decay of the IOZM spreading SST anomalies from western Indian Ocean to the eastern Indian Ocean. In contrast, in the Indian-Ocean Run, no oscillatory modes can be identified by the MSSA, even though the Indian Ocean SST variability is characterized by east–west SST contrast patterns similar to the IOZM. In both control and anomaly runs, IOZM-like SST variability appears to be associated with forcings from fluctuations of the Indian monsoon. Our modeling results suggest that the oscillatory feature of the IOZM is primarily forced by ENSO.

1. Introduction

The recent interests in the observed east–west contrast pattern in Indian Ocean sea-surface temperature (SST) anomalies have prompted the suggestion that the Indian Ocean has its own unstable coupled atmosphere-ocean mode like El Niño-Southern Oscillation (ENSO) (e.g., Saji et al, 1999; Webster et al, 1999). This interannual SST variability is often referred to as Indian Ocean Zonal Mode (IOZM) or Indian Ocean Dipole. The IOZM is characterized by opposite polarities of SST anomalies between the western and eastern parts of the equatorial Indian Ocean, and is accompanied with zonal wind anomalies in the central Indian Ocean. The strong wind-SST coupling associated with the IOZM has been used to argue for the similarity of the phenomenon to the delayed oscillator of ENSO (Webster et al, 1999). The fact that the temporal correlation between the observed IOZM and ENSO events is not strong and that several significant IOZM events have occurred in the absence of large ENSO events have lead to the suggestion that the IOZM is independent of ENSO (Saji et al, 1999). On the other hand, there are suggestions that the IOZM is not an

Effect of urbanization on the diurnal rainfall pattern in Houston

Steven J. Burian[1]* and J. Marshall Shepherd[2]

[1] *Department of Civil and Environmental Engineering, University of Utah, 122 S. Central Campus Drive, Suite 104, Salt Lake City, UT 84112, USA*
[2] *Earth Science Enterprise, NASA Goddard Space Flight Center, Greenbelt, MD 20771, USA*

Abstract:

Data from 19 raingauges located within and nearby Houston were analysed to quantify the impact of urbanization of the Houston metropolitan area on the local diurnal rainfall pattern. The average annual and warm-season diurnal rainfall patterns were determined for one time period when Houston was relatively small and likely would not have had a significant effect on meteorological processes (1940–58) and for a second, more recent, time period after Houston had become a major metropolitan area (1984–99). The diurnal rainfall patterns within the hypothesized urban-affected region and an upwind control region were compared for the pre- and post-urban time periods. Results indicated that the diurnal rainfall distribution in the urban area is much different than that found for the upwind and downwind adjacent regions for the 1984 to 1999 time period. For an average warm season from 1984 to 1999, the urban area and downwind urban-impacted region registered 59% and 30% respectively greater rainfall amounts from noon to midnight than an upwind control region. Moreover, the urban area had approximately 80% more recorded rainfall occurrences between noon and midnight during the warm season than surrounding areas. Comparison of the pre- and post-urban rainfall patterns indicated that the diurnal rainfall distribution has changed in southeast Texas. The changes are most significant in the urban area, especially for the afternoon time increments during the warm season. The average warm-season rainfall amount registered in the urban area increased by 25% from the pre- to the post-urban time period, while the amount in the upwind control region decreased by 8%. The majority of the increase was observed for the noon to 4 p.m. and 4 p.m. to 8 p.m. time increments. Copyright © 2005 John Wiley & Sons, Ltd.

KEY WORDS   inadvertent weather modification; urbanization; diurnal rainfall distribution

INTRODUCTION

Urbanization alters the appearance of the natural landscape and perturbs Earth system processes. The hydrological cycle, in particular, is changed during construction as vegetation is removed, the soil layer is modified, and built structures and drainage infrastructure are introduced. In general, development activities within a watershed will reduce infiltration and groundwater recharge, increase surface runoff volumes and rates, reduce soil moisture, and modify the spatial distribution and magnitude of surface storage and fluxes of water and energy. The perturbed post-development hydrological processes can contribute to increased frequencies and magnitudes of nuisance and severe floods, accelerated geomorphologic changes to downstream waterways, and aquatic habitat impacts. Urban drainage controls are designed and constructed to mitigate hydrological impacts of development. Design procedures are based on providing adequate conveyance, infiltration, and/or storage capacity to control the modified surface runoff produced by rainstorms. The change in watershed characteristics between pre- and post-development is included in the design by performing the runoff calculations for post-development conditions. However, the change in the rainfall characteristics possibly caused by urbanization is not accounted for in the traditional design process, whereby the design storm is

* Correspondence to: Steven J. Burian, Department of Civil and Environmental Engineering, University of Utah, 122 S Central Campus Drive, Suite 104, Salt Lake City, UT 84112, USA. E-mail: burian@eng.utah.edu

The Cold Front of 15 April 1994 over the Central United States. Part I: Observations

B. B. Demoz,* D. O'C. Starr,* K. D. Evans,[+] A. R. Lare,[#] D. N. Whiteman,* G. Schwemmer,*
R. A. Ferrare,[@] J. E. M. Goldsmith,[&] AND S. E. Bisson[&]

*NASA Goddard Space Flight Center, Greenbelt, Maryland
[+]University of Maryland, Baltimore County, Baltimore, Maryland
[#]L-3 Communications Government Services, Inc., Chantilly, Virginia
[@]NASA Langley Research Center, Hampton, Virginia
[&]Sandia National Laboratory, Livermore, California

ABSTRACT

Detailed observations of the interactions of a cold front and a dryline over the central United States that led to dramatic undulations in the boundary layer, including an undular bore, are investigated using high-resolution water vapor mixing ratio profiles measured by Raman lidars. The lidar-derived water vapor mixing ratio profiles revealed the complex interaction between a dryline and a cold-frontal system. An elevated, well-mixed, and deep midtropospheric layer, as well as a sharp transition (between 5- and 6-km altitude) to a drier region aloft, was observed. The moisture oscillations due to the undular bore and the mixing of the prefrontal air mass with the cold air at the frontal surface are all well depicted. The enhanced precipitable water vapor and roll clouds, the undulations associated with the bore, the strong vertical circulation and mixing that led to the increase in the depth of the low-level moist layer, and the subsequent lifting of this moist layer by the cold-frontal surface, as well as the feeder flow behind the cold front, are clearly indicated.

A synthesis of the Raman lidar–measured water vapor mixing ratio profiles, satellite, radiometer, tower, and Oklahoma Mesonet data indicated that the undular bore was triggered by the approaching cold front and propagated south-southeastward. The observed and calculated bore speeds were in reasonable agreement. Wave-ducting analysis showed that favorable wave-trapping mechanisms existed; a low-level stable layer capped by an inversion, a well-mixed midtropospheric layer, and wind curvature from a low-level jet were found.

1. Introduction

During evenings and early morning hours, the lower atmosphere commonly acts as a waveguide for the propagation of a variety of atmospheric waves that occur in a wide range of both temporal and spatial scales. The undular bore, a propagating disturbance characterized by an abrupt increase in ground-level pressure associated with an increase in ground-level temperature and a shift in wind direction often consisting of wavelike oscillations, is one example that uses the stably stratified layer within the lower atmosphere as a waveguide. Observations of bores have been reported by several authors including Clarke et al. (1981), Shreffler and Binkowski (1981), Smith et al. (1982),

Corresponding author address: Belay B. Demoz, NASA GSFC, Code 912, Greenbelt, MD 20771.
E-mail: belay.b.demoz@nasa.gov

Doviak and Ge (1984), Haase and Smith (1984), Simpson (1987), Cheung and Little (1990), Fulton et al. (1990), Koch et al. (1991), Locatelli et al. (1998), Koch and Clark (1999), and others. The Morning Glory, a frequent phenomenon near the Gulf of Carpentaria in northern Australia, reported extensively by Clarke et al. (1981), is an undular bore propagating along a temperature inversion generated by the interaction of a sea-breeze front with a nocturnal maritime inversion.

Several theories have been proposed as possible generation mechanisms for atmospheric bores. Numerical computations of density currents encountering strong stratification near the ground (Crook and Miller 1985; Crook 1986, 1988; Noonan and Smith 1986; Haase and Smith 1989), cool air behind colliding gravity currents (Clarke 1983; Noonan and Smith 1986; Wakimoto and Kingsmill 1995), thunderstorm outflows (Shreffler and Binkowski 1981; Doviak et al. 1989; Fulton et al. 1990), and mesoscale fronts (Smith et al. 1982; Koch et al.

Height distribution between cloud and aerosol layers from the GLAS spaceborne lidar in the Indian Ocean region

William D. Hart,[1] James D. Spinhirne,[2] Steven P. Palm,[1] and Dennis L. Hlavka[1]

[1] The Geoscience Laser Altimeter System (GLAS), a nadir pointing lidar on the Ice Cloud and land Elevation Satellite (ICESat) launched in 2003, now provides important new global measurements of the relationship between the height distribution of cloud and aerosol layers. GLAS data have the capability to detect, locate, and distinguish between cloud and aerosol layers in the atmosphere up to 40 km altitude. The data product algorithm tests the product of the maximum attenuated backscatter coefficient $b'(r)$ and the vertical gradient of $b'(r)$ within a layer against a predetermined threshold. An initial case result for the critical Indian Ocean region is presented. From the results the relative height distribution between collocated aerosol and cloud shows extensive regions where cloud formation is well within dense aerosol scattering layers at the surface. **Citation:** Hart, W. D., J. D. Spinhirne, S. P. Palm, and D. L. Hlavka (2005), Height distribution between cloud and aerosol layers from the GLAS spaceborne lidar in the Indian Ocean region, *Geophys. Res. Lett.*, *32*, L22S06, doi:10.1029/ 2005GL023671.

1. Introduction

[2] Both cloud and aerosols have important direct effects on the radiation balance of the earth. They influence the incoming solar energy by changing the albedo of the earth-atmosphere system and if absorbing they provide an increase in atmospheric radiative heating rates through the vertical range of their distribution. In addition, cloud and aerosol particles can interact with each other to produce significant secondary influences. For instance, *Twomey* [1974] describes how certain types of aerosols can increase low-cloud droplet concentrations, which would reduce incoming energy by increasing albedo without reducing the compensatory thermally emitted energy as much, and hence would be a cooling influence. More recent modeling studies [*Ackerman et al.*, 2003] support this theory while some satellite observations [*Platnick et al.*, 2000] seem to counter it. Opposed to the enhancement of low cloud cover by aerosol layers, there is evidence [*Ackerman et al.*, 2000] that heating by aerosol particles such as soot can reduce low cloud cover by absorbing incoming solar radiation. This is done both by evaporating cloud particles and stabilizing the boundary layer by preferred heating of its top. The interaction between aerosol and clouds are now also thought to be a major influence on precipitation [*Rosenfeld*, 2000].

[3] These examples of the opposing influences that the presence of aerosol has on the distribution and characteristics of cloud cover serve to illustrate the complexity of the atmospheric cloud-aerosol system. In order to quantify the effects that they impose on the earth's radiation balance, it is necessary that the global distribution of clouds and aerosol layers, especially with regard to their coincident occurrences, be well known. The height distribution of aerosol radiative forcing needs to be known separately and with correct clearing of cloud scattering [*Coakley et al.*, 2002]. In addition, the height distribution is an issue for the remote sensing of clouds. If there is significant aerosol scattering and absorption above cloud or elevated within clouds, passive multi-spectral techniques may be in error [*Sekiguchi et al.*, 2003]. Satellite observations provide a potential opportunity to find these distributions globally if the signals from the aerosols and clouds can be separated and vertically located. Spaceborne lidar offers a means to derive these kinds of products from backscatter measurements.

[4] The Geoscience Laser Altimeter System (GLAS) is a laser remote sensing instrument launched into orbit aboard ICESat in January, 2003. GLAS is a dual-purpose laser instrument, serving as both a precision surface elevation altimeter and atmospheric lidar [*Spinhirne et al.*, 2005]. Since February of 2003, GLAS has operated during discrete periods of approximately 33 days duration. When operating, it provides continuous and nearly pole-to-pole atmospheric lidar observations of clouds and aerosols through altitudes of 0–40km. A complete description of cloud and aerosol observations and analysis resolutions is given by *Palm et al.* [2002]. GLAS is sensitive to very optically rarefied particulate layers, down to backscatter cross section below 10^{-7} $(m\text{-}sr)^{-1}$ and is capable of detecting multiple layers to the limit of signal (optical depth < about 4.0).

[5] In this study, we introduce and present a brief summary of the GLAS cloud/aerosol algorithm. We show and discuss its strengths and weaknesses. Building on that, we present a case study in the heavily polluted Indian Ocean Region for the distribution of aerosol and clouds. We show GLAS's unique capability as a tool to accurately and comprehensively detect cloud and aerosols in the atmosphere and define their relative distribution.

2. Cloud/Aerosol Discrimination Technique

[6] A lidar signal is proportional to the attenuated backscatter coefficient, $b'(r)$. This is light backscattered from an atmospheric volume a distance r from the lidar multiplied by the intervening two way transmission. The GLAS cloud/aerosol detection and discrimination is based upon historically observed differences between cloud and aerosol layers in the magnitude of $b'(r)$, and the magnitude

---
[1]Science Systems and Applications, Inc., NASA Goddard Space Flight Center, Code 613.1, Greenbelt, Maryland, USA.
[2]NASA Goddard Space Flight Center, Code 613.1, Greenbelt, Maryland, USA.

Measurements of Ocean Surface Backscattering Using an Airborne 94-GHz Cloud Radar—Implication for Calibration of Airborne and Spaceborne W-Band Radars

LIHUA LI

Goddard Earth Sciences and Technology Center, University of Maryland, Baltimore County, Baltimore, Maryland

GERALD M. HEYMSFIELD

NASA Goddard Space Flight Center, Greenbelt, Maryland

LIN TIAN

Goddard Earth Sciences and Technology Center, University of Maryland, Baltimore County, Baltimore, Maryland

PAUL E. RACETTE

NASA Goddard Space Flight Center, Greenbelt, Maryland

ABSTRACT

Backscattering properties of the ocean surface have been widely used as a calibration reference for airborne and spaceborne microwave sensors. However, at millimeter-wave frequencies, the ocean surface backscattering mechanism is still not well understood, in part, due to the lack of experimental measurements. During the Cirrus Regional Study of Tropical Anvils and Cirrus Layers-Florida Area Cirrus Experiment (CRYSTAL-FACE), measurements of ocean surface backscattering were made using a 94-GHz (W band) cloud radar on board a NASA ER-2 high-altitude aircraft. This unprecedented dataset enhances our knowledge about the ocean surface scattering mechanism at 94 GHz. The measurement set includes the normalized ocean surface cross section over a range of the incidence angles under a variety of wind conditions. It was confirmed that even at 94 GHz, the normalized ocean surface radar cross section, σ_o, is insensitive to surface wind conditions near a $10°$ incidence angle, a finding similar to what has been found in the literature for lower frequencies. Analysis of the radar measurements also shows good agreement with a quasi-specular scattering model at low incidence angles. The results of this work support the proposition of using the ocean surface as a calibration reference for airborne millimeter-wave cloud radars and for the ongoing NASA CloudSat mission, which will use a 94-GHz spaceborne cloud radar for global cloud measurements.

1. Introduction

Clouds play a critical role in the earth's climate system. The vertical structure and spatial distributions of clouds are important in determining the earth's radiation budgets, which affect global circulations and ulti-mately climate. However, the lack of finescale cloud data is apparent in current climate model simulations (Houghton et al. 1995; Stephens et al. 1990). Millimeter-wave cloud radars have gained favor for measuring the spatial distribution of clouds because of their high scattering efficiency, low power consumption, and compact size. A number of airborne millimeter-wave cloud radars have been developed (Pazmany et al. 1994; Sadowy et al. 1997; Li et al. 2004). Meanwhile, a 94-GHz spaceborne cloud radar is in preparation for the National Aeronautics and Space Administration's

Corresponding author address: Lihua Li, NASA Goddard Space Flight Center, Code 912, Bldg. 33, Rm. C426, Greenbelt, MD 20771.
E-mail: lihua@agnes.gsfc.nasa.gov

Nucleation in synoptically forced cirrostratus

R.-F. Lin,[1,2] D. O. Starr,[3] J. Reichardt,[4] and P. J. DeMott[5]

[1] Formation and evolution of cirrostratus in response to weak, uniform, and constant synoptic forcing is simulated using a one-dimensional numerical model with explicit microphysics, in which the particle size distribution in each grid box is fully resolved. A series of tests of the model response to nucleation modes (homogeneous-freezing-only/heterogeneous nucleation) and heterogeneous nucleation parameters are performed. In the case studied here, nucleation is first activated in the prescribed moist layer. A continuous cloud-top nucleation zone with a depth depending on the vertical humidity gradient and one of the nucleation parameters is developed afterward. For the heterogeneous nucleation cases, intermittent nucleation zones in the mid-upper portion of the cloud form where the relative humidity is on the rise because existent ice crystals falling from higher nucleation zones do not efficiently deplete the excess water vapor and ice nuclei are available. Vertical resolution as fine as 1 m is required for realistic simulation of the homogeneous-freezing-only scenario, while the model resolution requirement is more relaxed in the cases where heterogeneous nucleation dominates. Bulk microphysical and optical properties are evaluated and compared. Ice particle number flux divergence, which is due to the vertical gradient of the gravity-induced particle sedimentation, is constantly and rapidly changing the local ice number concentration, even in the nucleation zone. When the depth of the nucleation zone is shallow, particle number concentration decreases rapidly as ice particles grow and sediment away from the nucleation zone. When the depth of the nucleation zone is large, a region of high ice number concentration can be sustained. The depth of nucleation zone is an important parameter to be considered in parametric treatments of ice cloud generation.

Citation: Lin, R.-F., D. O. Starr, J. Reichardt, and P. J. DeMott (2005), Nucleation in synoptically forced cirrostratus, *J. Geophys. Res.*, *110*, D08208, doi:10.1029/2004JD005362.

1. Introduction

[2] The optical depth of cirrus, one of the controlling factors determining its associated net cloud radiative forcing, depends on the cloud ice water path (IWP) and effective particle size [e.g., *Foot*, 1988]. Some state-of-the-art general circulation models (GCMs) now predict hydrometeor mixing ratios [e.g., *Del Genio et al.*, 1996; *Fowler et al.*, 1996]. However, realistic prediction of cirrus optical and microphysical properties requires accurate estimation of the number concentration of ice particles generated in the nucleation regime. Using an approximate analytical solution validated by parcel model simulations, *Kärcher and Lohmann* [2002] developed a parameterization scheme for ice particle number concentration via homogeneous freezing nucleation of aerosol particles and implemented it into the European Center Hamburg (ECHAM) GCM [*Lohmann and Kärcher*, 2002] to examine the aerosol effects on the ice cloud and Earth-atmosphere radiative budgets. Despite advances in parameterization schemes of aerosol effects on ice initiation, our fundamental understanding of the evolution of synoptically forced cirrus still lags. Studies based on parcel models are typically not able to provide information about the entire cloud from cloud base to cloud top. Moreover, parcel model studies usually assume that the ice particles are lifted with the parcel (no particle fallout or fall-in) and that there is no exchange of mass or heat with the environment. Neglect of particle fallout/fall-in is questionable for weak forcing conditions, where nucleation may last several to more than 10 min. Thus a model of one-dimension (1-D) or higher [e.g., *Jensen et al.*, 1994a, 1994b; *Khvorostyanov et al.*, 2001; *Sassen et al.*, 2002] is needed to adequately estimate cloud bulk properties over the entire cloud depth. In our study a 1-D model with an explicit microphysical scheme is used to simulate a column of air lifted by a gentle updraft.

---

[1]Goddard Earth Sciences and Technology Center, University of Maryland Baltimore County, Baltimore, Maryland, USA.
[2]Also at Laboratory for Atmospheres, NASA Goddard Space Flight Center, Greenbelt, Maryland, USA.
[3]Laboratory for Atmospheres, NASA Goddard Space Flight Center, Greenbelt, Maryland, USA.
[4]DWD-Meteorologisches Observatorium Lindenberg, Tauche, Germany.
[5]Department of Atmospheric Science, Colorado State University, Fort Collins, Colorado, USA.

Validation of ECMWF global forecast model parameters using GLAS atmospheric channel measurements

Stephen P. Palm,[1] Angela Benedetti,[2] and James Spinhirne[3]

[1]   Satellite lidar (LIght Detection And Ranging) data from GLAS is used to ascertain the performance of the European Center for Medium Range Weather Forecasts model predictions of cloud fraction, cloud vertical distribution, and boundary layer height. Results show that the model is reasonably accurate for low and middle clouds, but often misses the location and amount of high cirrus clouds. The model tends to overestimate high cloud fraction and this error grows with forecast length. The GLAS-derived boundary layer height over the oceans is generally 200–400 m higher than the model predictions, but small-scale and global patterns of PBL height show similar features. **Citation:** Palm, S. P., A. Benedetti, and J. Spinhirne (2005), Validation of ECMWF global forecast model parameters using GLAS atmospheric channel measurements, *Geophys. Res. Lett.*, *32*, L22S09, doi:10.1029/2005GL023535.

1.   Introduction

[2]   In January 2003 the Geoscience Laser Altimeter System (GLAS) was launched into a near-polar orbit aboard the Ice Cloud and land Elevation Satellite (ICESat) [*Zwally et al.*, 2002]. In addition to a high resolution 1064 nm altimetry channel, GLAS contains both 1064 and 532 nm atmospheric backscatter lidar channels. The 532 nm atmospheric channel has been operating since September 25, 2003 providing unprecedented views of the vertical structure of atmospheric aerosol, cloud layers and the depth and structure of the planetary boundary layer (PBL) [*Spinhirne et al.*, 2005]. The high vertical (76 m) and horizontal (175 m) resolution of the GLAS data provide accurate measurements of cloud height and vertical structure, tropopause height and Planetary Boundary Layer (PBL) height. These measurements constitute a valuable data set for the validation of global weather forecast and climate models. Clouds play an integral role in the climate system, primarily through their role as modulators of radiative transfer and their contribution to diabatic heating. The accurate representation of clouds in these models is, therefore, extremely important. However, it is difficult, if not impossible, to verify its forecasts of cloud extent and coverage, especially in the vertical. Similarly, PBL height is an important model parameter that is difficult to validate due to a lack of global observations.

[3]   GLAS represents a unique opportunity to verify cloud field forecasts of various models such as the European Center for Medium-range Weather Forecasts (ECMWF) forecast model. Using an approach similar to the method presented here, *Miller et al.* [1999] validated ECMWF model output of cloud height and coverage using limited data from the shuttle Lidar In-space Technology Experiment (LITE). *Randall et al.* [1998] compared boundary layer height derived from the LITE data with output from the Colorado State University atmospheric general circulation model as well as the National Center for Atmospheric Research (NCAR) Community Climate Model 3 (CCM3). In this paper we demonstrate the utility of GLAS data for the verification of global ECMWF output fields of cloud height, fraction and PBL height. As orbiting lidar data from the ICESat Mission, CALIPSO [*Winker et al.*, 2003] and The Earth Explorer Atmospheric Dynamics Mission (ADM-Aeolus) [*Duran et al.*, 2004] and those to follow become commonplace, the value for not only model validation but also for data assimilation will greatly increase.

2.   Data and Methodology

[4]   The ECMWF spectral model contains a sophisticated cloud scheme that is highly regarded within the scientific community [*Jakob*, 2003]. It uses triangular truncation at wave number 511 (roughly 40 km resolution) and has 60 model levels in the vertical. This is a slight increase in resolution compared to the version of the ECMWF model used by *Miller et al.* [1999] in their analyses (60×60 km horizontal with 31 vertical levels). The GLAS data utilized for this study are the vertical cross-sections of calibrated attenuated backscatter along the ICESat ground track (GLA07) [*Spinhirne et al.*, 2005]. The 5 Hz data were first averaged to a 5 second horizontal resolution (35 km), and the 5s orbital position data were then supplied to ECMWF for a number of ICESat orbits. ECMWF 6 and 48 hour global forecasts were run such that the verification times are within 3 hours of the given ICESat orbit. The ECMWF forecast fields were extracted from the output grid box that intersects with the ICESat orbit. The ECMWF data consist of vertical profiles of the prognostic fields at each of 60 model pressure levels ranging from the surface to the 0.1 mb level, where each pressure surface corresponds to a specific geometric height. Linear interpolation was then used to vertically interpolate the ECMWF cloud fraction from the model levels to the vertical grid defined by the GLAS data (every 76 m) starting at sea level and extending to an altitude of 20 km. After this process is completed, the two data sets are vertically aligned and can be compared in a number of ways. Note that in the analysis presented here, no consideration is being made for the fact that we are comparing a thin cross-section through the atmosphere with

---

[1]Science Systems and Applications Inc., Lanham, Maryland, USA.
[2]European Center for Medium Range Weather Forecasts, Reading, UK.
[3]Goddard Space Flight Center, Greenbelt, Maryland, USA.

Cloud and aerosol measurements from GLAS: Overview and initial results

James D. Spinhirne,[1] Stephen P. Palm,[2] William D. Hart,[2] Dennis L. Hlavka,[2] and Ellsworth J. Welton[1]

[1] Global space borne lidar profiling of atmospheric clouds and aerosol began in 2003 following the launch of the Geoscience Laser Altimeter System (GLAS) on the Ice, Cloud and land Elevation Satellite. GLAS obtains nadir profiles through the atmosphere in two wavelength channels, day and night, at a fundamental resolution of 76.8 m vertical and 172 m along track. The 532 nm channel uses photon-counting detectors and resolves profiles of observed backscatter cross sections to 10^{-7} 1/m-sr. The 1064 nm channel employs analog detection adequate to 10^{-6} 1/m-sr and with greater dynamic range. By 2005 approximately seven months of global data are available. Processing algorithms produce data products for the corrected lidar signal, cloud and aerosol layer boundaries and optical thickness and extinction and backscatter cross sections. Operational sensitivity is shown by the frequency distribution for cloud optical thickness peaking at approximately 0.02. **Citation:** Spinhirne, J. D., S. P. Palm, W. D. Hart, D. L. Hlavka, and E. J. Welton (2005), Cloud and aerosol measurements from GLAS: Overview and initial results, *Geophys. Res. Lett.*, *32*, L22S03, doi:10.1029/2005GL023507.

1. Introduction

[2] Since the advent of satellite remote-sensing, passive imaging radiometers of multiple types have provided observations of global cloud and aerosol layer distributions. Yet there are issues of increasing importance where passive sensing alone is not adequate. Both cloud feedback and the influence of aerosol are considered major uncertainties for predictions of global warming. Global observations should be sufficient to provide adequate information for climate models, but also of sufficient sensitivity to monitor critical component variability in response to climate change. Passive instruments do not provide direct and accurate observations of the height distribution of aerosol along with accurate extinction and absorption information. Similarly for cloud cover, errors in height and coverage from passive retrieval are typically large in comparison to the impact on infrared forcing from increasing greenhouse gasses. Active laser remote sensing of the atmosphere has the major advantage of a direct and unambiguous detection and height measurement of all scattering layers, and thus space borne lidar observations will be an important addition to existing satellite observations.

[3] The first polar-orbiting satellite lidar instrument, the Geoscience Laser Altimeter System (GLAS), was launched on board the Ice, Cloud and land Elevation Satellite in January 2003 and has provided extensive global data on cloud and aerosol distributions. As part of the NASA Earth Observing System (EOS) project, the GLAS instrument is intended as a laser sensor fulfilling complementary requirements for several earth science disciplines [*Zwally et al.*, 2002; *Spinhirne and Palm*, 1996]. The overall approach takes advantage of the good technical compatibility of cloud and aerosol profiling with laser altimeter measurements for ice sheet and land requirements. In addition, a mission that combines surface altimetry and high quality atmospheric measurements best overcomes inter related remote sensing problems such as the effect of cloud scattering on precision altimetry [*Duda et al.*, 2001].

[4] In this paper we present an initial description of the GLAS atmospheric observations. Specific examples of the application of GLAS data to a range of issues are given in this special section [*Hlavka et al.*, 2005; *Palm et al.*, 2005a, 2005b; *Spinhirne et al.*, 2005; *Hart et al.*, 2005]. The stated measurement requirement for GLAS was to profile all radiative significant cloud and aerosol layers. The measurement result from the fully operational instrument meets the requirement. An important part of the development of the GLAS project was the construction and testing of automated data processing algorithms capable of operational production of higher-level research parameters. We describe the GLAS cloud and aerosol data products available to the science community, starting September 2004.

2. GLAS Observation Requirements and Examples

[5] The lidar measurement requirements for clouds and aerosol from space were based on a long experience with airborne and ground based observations. The stated requirement to profile all significant cloud and aerosol translates to detection at appropriate spatial resolution of layers of optical depth down to 0.01. The requirement then further translates to the observation of backscattering cross sections to below 10^{-7} 1/m-sr. Airborne observations indicate that there is a "background" aerosol mode into the troposphere with cross sections at visible wavelengths on the order of $10^{-9}-10^{-8}$ 1/m-sr [*Menzies et al.*, 2002]. Thus some aerosol concentrations exist below the stated measurement requirement, but these aerosol are considered below the definition of radiative significant.

[6] The GLAS instrument is a dual-frequency, nadir-viewing laser radar system (J. Abshire et al., Geoscience Laser Altimeter System (GLAS) on the ICESat mission:

[1]NASA Goddard Space Flight Center, Greenbelt, Maryland, USA.
[2]Science Systems and Applications Inc., Lanham, Maryland, USA.

Ground Validation for the Tropical Rainfall Measuring Mission (TRMM)

DAVID B. WOLFF,[*,+] D. A. MARKS,[*,#] E. AMITAI,[*,#] D. S. SILBERSTEIN,[*,#] B. L. FISHER,[*,+]
A. TOKAY,[*,@] J. WANG,[*,+] AND J. L. PIPPITT[*,#]

Laboratory for Atmospheres, NASA Goddard Space Flight Center, Greenbelt, Maryland
+*Science Systems & Applications, Inc., Lanham, Maryland*
#*Center for Earth Observing and Space Research, George Mason University, Fairfax, Virginia*
@*Joint Center for Earth Systems Technology, University of Maryland, Baltimore County, Baltimore, Maryland*

ABSTRACT

An overview of the Tropical Rainfall Measuring Mission (TRMM) Ground Validation (GV) Program is presented. This ground validation (GV) program is based at NASA Goddard Space Flight Center in Greenbelt, Maryland, and is responsible for processing several TRMM science products for validating space-based rain estimates from the TRMM satellite. These products include gauge rain rates, and radar-estimated rain intensities, type, and accumulations, from four primary validation sites (Kwajalein Atoll, Republic of the Marshall Islands; Melbourne, Florida; Houston, Texas; and Darwin, Australia). Site descriptions of rain gauge networks and operational weather radar configurations are presented together with the unique processing methodologies employed within the Ground Validation System (GVS) software packages. Rainfall intensity estimates are derived using the Window Probability Matching Method (WPMM) and then integrated over specified time scales. Error statistics from both dependent and independent validation techniques show good agreement between gauge-measured and radar-estimated rainfall. A comparison of the NASA GV products and those developed independently by the University of Washington for a subset of data from the Kwajalein Atoll site also shows good agreement. A comparison of NASA GV rain intensities to satellite retrievals from the TRMM Microwave Imager (TMI), precipitation radar (PR), and Combined (COM) algorithms is presented, and it is shown that the GV and satellite estimates agree quite well over the open ocean.

---

1. Introduction

The Tropical Rainfall Measuring Mission (TRMM) is a satellite-based program to measure tropical rainfall and to help quantify the associated distribution and transport of latent heat, which drives the global atmospheric system. TRMM is a joint United States–Japan mission launched from Tanegashima, Japan, on 27 November 1997 (Simpson et al. 1996; Kummerow et al. 1998). TRMM has provided state-of-the-art precipitation measurements since shortly after launch and was boosted from its original 350-km orbit to a new orbit of 402.5 km in August 2001 in order to extend science observations beyond the original time frame of 2000. A key effort of TRMM has been dedicated to providing ground validation (GV) of the satellite rainfall estimates. The GV program is based in the TRMM Satellite Validation Office (TSVO) at the NASA Goddard Space Flight Center (GSFC) in Greenbelt, Maryland.

The GV program has been collecting radar and rain gauge measurements since 1988 and continues to collect datasets at a number of sites located throughout the Tropics.

The aim of this paper is to provide a summary of GV operations, algorithm descriptions, and data quality. A description of the primary GV sites and details of their operational configurations, including a description of the network of radar and rain gauge networks at each site, are provided in section 2. Section 3 discusses the software system and algorithms developed and maintained by TSVO for processing the data, details data sources and ingest methodologies, and provides a brief description of the level I–III TRMM GV Science Products (TSP) and how they are produced. Section 4 provides a discussion on the error statistics of the radar rainfall estimates versus both dependent and independent gauge measurements, as well as a comparison of rain rates and monthly accumulations between TSVO and those produced by the University of Washington. Section 5 provides validation comparisons between TRMM GV and satellite-retrieved rain intensities generated by the TRMM Microwave Imager (TMI), precipitation radar (PR), and Combined (COM) algorithms.

Corresponding author address: David B. Wolff, NASA GSFC, Code 912.1, Greenbelt, MD 20771.
E-mail: wolff@radar.gsfc.nasa.gov

Impacts of Air–Sea Interaction on Tropical Cyclone Track and Intensity

LIGUANG WU

*Goddard Earth and Technology Center, University of Maryland, Baltimore County, Baltimore, and Laboratory for Atmospheres,
NASA Goddard Space Flight Center, Greenbelt, Maryland*

BIN WANG

Department of Meteorology, School of Ocean and Earth Science and Technology, University of Hawaii at Manoa, Honolulu, Hawaii

SCOTT A. BRAUN

Laboratory for Atmospheres, NASA Goddard Space Flight Center, Greenbelt, Maryland

ABSTRACT

While the previous studies of the impacts of air–sea interaction on tropical cyclones (TCs) generally agree on significant reduction in intensity and little change in track, they did not further explore the relative roles of the weak symmetric and strong asymmetric sea surface temperature (SST) anomalies relative to the TC center. These issues are investigated numerically with a coupled hurricane–ocean model in this study.

Despite the relatively small magnitude compared to the asymmetric component of the resulting cooling, the symmetric cooling plays a decisive role in weakening TC intensity. A likely reason is that the symmetric cooling directly reduces the TC intensity, while the asymmetric cooling affects the intensity through the resulting TC asymmetries, which are mainly confined to the lower boundary and much weaker than those resulting from large-scale environmental influences.

The differences in TC tracks between the coupled and fixed SST experiments are generally small because of the competing processes associated with the changes in TC asymmetries and the beta drift induced by air–sea interaction. The symmetric component of the SST drop weakens the TC intensity and outer strength, leading to a more northward beta drift. On the other hand, since the asymmetric component of the SST cooling is negative in the rear and positive in the front of a TC in the coupled experiments, the enhanced diabatic heating is on the southern side of a westward-moving TC, tending to shift the TC southward. In the coupled model the westward TCs with relatively weak (strong) outer strength tend to turn to the north (south) of the corresponding TCs without air–sea interaction.

1. Introduction

A tropical cyclone (TC) develops and is maintained by drawing energy from the underlying ocean surface. It can form only over waters of 26°C or higher and its intensity is very sensitive to the sea surface temperature (SST; e.g., Tuleya and Kurihara 1982; Emanuel 1986). Treating a tropical storm as a Carnot heat engine, Emanuel (1986) suggested that the TC maximum po-

tential intensity is primarily determined by the underlying SST. At the same time, the surface wind stress associated with a TC can generate strong turbulent mixing that deepens the ocean mixed layer (OML) by entraining cooler water into the surface layer, leading to significant SST decreases. Observations indicate that the SST cooling caused by TCs ranges from 1° to 6°C (Price 1981).

The feedback of the resulting cooling on TC intensity has been investigated using coupled hurricane–ocean models. Early experiments were performed with upper OML models forced by axisymmetric TC models (Elsberry et al. 1976; Chang and Anthes 1979; Sutyrin and Khain 1979). Because of the markedly rightward bias of

Corresponding author address: Dr. Liguang Wu, NASA GSFC, Code 912, Greenbelt, MD 20771.
E-mail: liguang@agnes.gsfc.nasa.gov

ARTICLES

IMPROVING NATIONAL AIR QUALITY FORECASTS WITH SATELLITE AEROSOL OBSERVATIONS

BY JASSIM AL-SAADI, JAMES SZYKMAN,* R. BRADLEY PIERCE, CHIEKO KITTAKA, DOREEN NEIL, D. ALLEN CHU, LORRAINE REMER, LIAM GUMLEY, ELAINE PRINS,+ LEWIS WEINSTOCK, CLINTON MACDONALD, RICHARD WAYLAND, FRED DIMMICK, AND JACK FISHMAN

Satellite aerosol observations—which are particularly helpful in tracking long-range transport aloft—can overcome some of the limitations of surface monitoring networks and enhance daily air quality forecasts associated with particle pollution.

Public awareness of local air quality is growing rapidly. Air quality is often considered like the weather—it changes, and some days are better than others. While poor air quality impairs visibility and can damage vegetation and structures, most importantly it can cause serious health problems, including respiratory difficulties and even premature death. Accurate air quality forecasts can offer significant societal and economic benefits by enabling advance planning. Individuals can adjust their outdoor activities to minimize the adverse health impacts of poor air quality. The severity of local pollution episodes may even be reduced by allowing early implementation of mitigation procedures commonly referred to as "action days." Yet air quality forecasting is quite complex. While pollution episodes are typically associated with local meteorological conditions and nearby emissions, it is increasingly recognized

AFFILIATIONS: AL-SAADI, PIERCE, NEIL, AND FISHMAN—NASA Langley Research Center, Hampton, Virginia; SZYKMAN—Office of Research and Development, U.S. EPA, Research Triangle Park, North Carolina; KITTAKA—SAIC, Hampton, Virginia; CHU—Joint Center for Earth Science Technology, University of Maryland, Baltimore County, Baltimore, Maryland; REMER—NASA Goddard Space Flight Center, Greenbelt, Maryland; GUMLEY—SSEC/CIMSS, University of Wisconsin—Madison, Madison, Wisconsin; PRINS—NOAA/NESDIS/ORA, University of Wisconsin—Madison, Madison, Wisconsin; WEINSTOCK, WAYLAND, AND DIMMICK—Office of Air Quality Planning and Standards, U.S. EPA, Research Triangle Park, North Carolina; MACDONALD—Sonoma Technology, Inc., Petaluma, California
*CURRENT ASSIGNMENT: NASA Langley Research Center, Hampton, Virginia
+CURRENT AFFILIATION: SSEC/CIMSS, University of Wisconsin—Madison, Madison, Wisconsin
CORRESPONDING AUTHOR: Jassim Al-Saadi, MS 401B, NASA Langley Research Center, Hampton, VA 23681
E-mail: j.a.al-saadi@nasa.gov

THE I3RC

Bringing Together the Most Advanced Radiative Transfer Tools for Cloudy Atmospheres

by Robert F. Cahalan, Lazaros Oreopoulos, Alexander Marshak, K. Franklin Evans, Anthony B. Davis, Robert Pincus, Ken H. Yetzer, Bernhard Mayer, Roger Davies, Thomas P. Ackerman, Howard W. Barker, Eugene E. Clothiaux, Robert G. Ellingson, Michael J. Garay, Evgueni Kassianov, Stefan Kinne, Andreas Macke, William O'Hirok, Philip T. Partain, Sergei M. Prigarin, Alexei N. Rublev, Graeme L. Stephens, Frederic Szczap, Ezra E. Takara, Támas Várnai, Guoyong Wen, and Tatiana B. Zhuravleva

An international Intercomparison of 3D Radiation Codes (I3RC) underscores the vast progress of recent years, but also highlights the challenges ahead for routine implementation in remote sensing and global climate modeling applications.

odeling atmospheric and oceanic processes is one of the most important methods of the earth sciences for understanding the interactions of the various components of the surface–atmosphere system and predicting future weather and climate states. Great leaps in the availability of computing power at continuously decreasing costs have led to widespread popularity of computer models for research and operational applications. As part of routine scientific work, output from models built for

AFFILIATIONS: Cahalan—NASA Goddard Space Flight Center, Greenbelt, Maryland; Oreopoulos, Várnai, and Wen—University of Maryland, Baltimore County, Baltimore, and NASA Goddard Space Flight Center, Greenbelt, Maryland; Marshak—NASA Goddard Space Flight Center, Greenbelt, and University of Maryland, Baltimore County, Baltimore, Maryland; Evans—University of Colorado, Boulder, Colorado; Davis—Los Alamos National Laboratory, Los Alamos, New Mexico; Pincus—NOAA–CIRES Climate Diagnostics Center, Boulder, Colorado; Yetzer—Raytheon-ITSS, Beltsville, and NASA Goddard Space Flight Center, Greenbelt, Maryland; Mayer—Deutsches Zentrum für Luft und Raumfahrt, Oberpfaffenhofen, Germany; Davies—Jet Propulsion Laboratory, Pasadena, California; Ackerman and Kassianov—Pacific Northwest National Laboratory, Richland, Washington; Barker—Meteorological Service of Canada, Downsview, Ontario, Canada; Clothiaux—The Pennsylvania State University, University Park, Pennsylvania; Ellingson and Takara—The Florida State University, Tallahassee, Florida; Garay—University of California, Los Angeles, Los Angeles, California; Kinne—Max-Planck-Institut für Meteorologie, Hamburg, Germany; Macke—Liebniz Institute for Marine Sciences, IFM-GEOMAR, University of Kiel, Kiel, Germany; O'Hirok—University of California, Santa Barbara, Santa Barbara, California; Partain and Stephens—Colorado State University, Fort Collins, Colorado; Prigarin—Institute for Computational Mathematics and Mathematical Geophysics, Novosibirsk, Russia; Rublev—Kurchatov Institute, Moscow, Russia; Szczap—Université Blaise Pascal, Clermont-Ferrand, France; Zhuravleva—Institute of Atmospheric Optics, Tomsk, Russia

CORRESPONDING AUTHOR: Robert F. Cahalan, NASA GSFC, Code 613.2, Greenbelt, MD 20771
E-mail: Robert.F.Cahalan@nasa.gov

A Method to Derive Smoke Emission Rates From MODIS Fire Radiative Energy Measurements

Charles Ichoku and Yoram J. Kaufman

Abstract—Present methods of emissions estimation from satellite data often use fire pixel counts, even though fire strengths and smoke emission rates can differ by some orders of magnitude between pixels. Moderate Resolution Imaging Spectroradiometer (MODIS) measurements of fire radiative energy (FRE) release rates R_{fre} range from less than 10 to more than 1700 MW per pixel at 1-km resolution. To account for the effect of such a wide range of fire strengths/sizes on smoke emission rates, we have developed direct linear relationships between the MODIS-measured R_{fre} and smoke aerosol emission rates R_{sa} (in kilograms per second), derived by analyzing MODIS measurements of aerosol spatial distribution around the fires with National Center for Environmental Prediction/National Center for Atmospheric Research wind fields. We applied the technique to several regions around the world and derived a FRE-based smoke emission coefficient, C_e (in kilograms per megajoule), which can be simply multiplied by R_{fre} to calculate R_{sa}. This new coefficient C_e is an excellent remote sensing parameter expressing the emission strength of different ecosystems and regions. Analysis of all 2002 MODIS data from Terra and Aqua satellites yielded C_e values of 0.02–0.06 kg/MJ for boreal regions, 0.04–0.08 kg/MJ for both tropical forests and savanna regions, and 0.08–0.1 kg/MJ for Western Russian regions. These results are probably overestimated by about 50% because of uncertainties in some of the data, parameters, and assumptions involved in the computations. This 50% overestimation is comparable to uncertainties in traditional emission factors. However, our satellite method shows great promise for accuracy improvement, as better knowledge is gained about the sources of the uncertainties.

Index Terms—Aerosol, biomass burning, fire radiative energy (FRE), Moderate Resolution Imaging Spectroradiometer (MODIS), particulate matter, smoke emission.

I. INTRODUCTION

WILDFIRES and prescribed biomass-burning devastate vast areas of forest lands, grass lands, and agricultural lands across the globe, consuming an estimated 5500–9200 Tg of biomass annually [1], [2]. For instance, in Canada alone, it was estimated that about 4.9 million hectares burned in 1995 [3]. By so doing, fires directly exert adverse (and, in some cases, favorable) influences on ecology, population, habitat,

agriculture, transportation, and security. The 2001 report of the Intergovernmental Panel on Climate Change (IPCC) [4] states that "most climate scenarios indicate that the probability of large fires will increase" (IPCC, 2001, sec 13.2.2.1.2). The effects of fires on climate and the environment are not limited to the ravages of their flame but also include the impacts of the energy, aerosols (or particulate matter, PM), and trace gases emitted into the atmosphere. Fires release heat energy, which is propagated by conduction, convection, and radiation. Fire radiative energy (FRE), like other types of electromagnetic radiant energy, propagates in space and can be sensed from aircraft and satellites. The Moderate-Resolution Imaging Spectroradiometer (MODIS) sensor, launched aboard the Earth Observing System (EOS) Terra and Aqua satellites on December 18, 1999 and May 4, 2002, respectively, is the first to operationally measure from space the FRE rate of release (R_{fre}), using its 3.96-μm channels, which do not saturate for most fires.

Commensurate with the large volumes of biomass consumed by fires, tremendous amounts of smoke are emitted into the atmosphere annually. Globally, an estimated 3.1×10^9 t of biomass carbon is exposed to burning annually, of which 1.1×10^9 t is emitted to the atmosphere through combustion [5]. Smoke comprises aerosol particles and trace gases (including CO_2, CO, CH_4, and other species), which constitute air pollutants and contribute to the perturbation of the global radiative balance through the scattering and absorption of solar radiation. Andreae and Merlet [6] provide a detailed list of the various particulate and gaseous species emitted by fires. Although some trace gases (CO_2 and CH_4) have long been associated with climate change, atmospheric aerosols and, particularly, smoke aerosol (because of its considerable black carbon content) probably have a much greater impact, not only on climate, but also on weather, health, aviation, visibility, and environmental pollution. However, the global effects of fires and emitted smoke aerosols and trace gases are still poorly understood. To fully understand the effects of biomass burning on humans and the environment, it is important to acquire an accurate quantitative inventory of the fire locations and frequency, the amount of biomass they consume, and the energy, aerosols, and trace gases they release into the atmosphere.

Accurate assessment of the environmental and climate effects of smoke can only be achieved if the amount or the rate of emission of smoke is estimated accurately. It is a common saying that: "there is no smoke without fire." Ironically, some of the initial attempts at estimating emissions did not include any quantitative measure of the fire, but were based on limited localized smoke measurements, which were then extrapolated

MEETING SUMMARIES

INCLUSION OF URBAN LANDSCAPE IN A CLIMATE MODEL
How Can Satellite Data Help?

BY MENGLIN JIN AND J. MARSHALL SHEPHERD

Urban regions, which cover only approximately 0.2% of the earth's land surface, contain about half of the human population (UNPD 2001). Modeling urban weather and climate is critical for human welfare, but has been hampered for at least two reasons: i) no urban landscape has been included in global and regional climate models (GCMs and RCMs, respectively), and ii) detailed information on urban characteristics is hard to obtain. With the advance of satellite observations, adding urban schemes into climate models in order to scale projections of global/regional climate to urban areas becomes essential. Inclusion of urbanized landscape into climate models was discussed in depth at the fall American Geophysical Union (AGU) meeting of 2003 in the session entitled "Human-induced climate variations linked to urbanization: From observations to modeling," which took place on 12 December 2003 in San Francisco, California (most of the presentations of this session can be found online at www.atmos.umd.edu/~mjin/AGU03urban.html). The

AFFILIATIONS: JIN—Department of Meteorology, University of Maryland, College Park, College Park, Maryland; SHEPHERD—NASA Goddard Space Flight Center, Greenbelt, Maryland
CORRESPONDING AUTHOR: Dr. Menglin Jin, Department of Meteorology, University of Maryland, College Park, College Park, MD 20742
E-mail: mjin@atmos.umd.edu

> **AGU MEETING SESSION—HUMAN-INDUCED CLIMATE VARIATIONS LINKED TO URBANIZATION: FROM OBSERVATIONS TO MODELING**
>
> What: The unique radiative characteristics of urban land cover are now being observed by satellites, with consequent improvements possible in surface schemes of climate models
> When: 12 December 2003
> Where: San Francisco, California

following notes summarize what is known and what needs to be advanced on this topic.

In a GCM and RCM, land physical processes are simulated in a land surface model, which is coupled with the atmosphere model through exchanges of heat fluxes, water, and momentum. Currently, an urban classification is not included in any major GCM/RCM land surface model [e.g., the second National Center for Atmospheric Research (NCAR) Community Land Model (CLM2), National Aeronautics and Space Administration (NASA) Global Modeling and Assimilation Office (GMAO) unified land surface model, Biosphere–Atmosphere Transfer Scheme (BATS), simple Biosphere model, version 2 (SIB2), etc.]. This exclusion makes GCMs/RCMs inadequate for realistically simulating urban modifications to climate.

The same land surface model can be coupled to a GCM or RCM. For example, the NCAR CLM is coupled to both the NCAR community atmosphere

Aerosol anthropogenic component estimated from satellite data

Y. J. Kaufman,[1] O. Boucher,[2,3] D. Tanré,[4] M. Chin,[1] L. A. Remer,[1] and T. Takemura[1,5]

[1] Satellite instruments do not measure the aerosol chemical composition needed to discriminate anthropogenic from natural aerosol components. However the ability of new satellite instruments to distinguish fine (submicron) from coarse (supermicron) aerosols over the oceans, serves as a signature of the anthropogenic component and can be used to estimate the fraction of anthropogenic aerosols with an uncertainty of ±30%. Application to two years of global MODIS data shows that 21 ± 7% of the aerosol optical thickness over the oceans has an anthropogenic origin. We found that three chemical transport models, used for global estimates of the aerosol forcing of climate, calculate a global average anthropogenic optical thickness over the ocean between 0.030 and 0.036, in line with the present MODIS assessment of 0.033. This increases our confidence in model assessments of the aerosol direct forcing of climate. The MODIS estimated aerosol forcing over cloud free oceans is therefore -1.4 ± 0.4 W/m^2. **Citation:** Kaufman, Y. J., O. Boucher, D. Tanré, M. Chin, L. A. Remer, and T. Takemura (2005), Aerosol anthropogenic component estimated from satellite data, *Geophys. Res. Lett.*, *32*, L17804, doi:10.1029/2005GL023125.

1. Introduction

[2] Climate change research [*Intergovernmental Panel on Climate Change (IPCC)*, 2001] and studies of the aerosol forcing on the hydrological cycle [*Ramanathan et al.*, 2001] require knowledge of the anthropogenic component of the aerosol. Natural aerosols can cause variability in the climate system and be part of its feedbacks mechanisms, e.g. larger amount of dust generated during drought conditions in the Sahel [*Prospero and Lamb*, 2003] can cause cooling of the earth system and changes in the drought conditions. Only anthropogenic aerosol can be considered as an external cause of climate change [*Charlson et al.*, 1992]. Aerosol exerts a radiative forcing of climate via direct absorption and reflection of sunlight to space and via induced changes in the cloud microphysics, water content, and coverage [*Gunn and Phillips*, 1957; *Twomey et al.*, 1984; *Albrecht*, 1989; *Rosenfeld*, 2000; *Koren et al.*, 2004].

[3] Yet assessments of the aerosol radiative forcing [*IPCC*, 2001] are based only on models since we do not have a method to measure the amount and distribution of anthropogenic aerosol around the Earth. Previously [*Kaufman et al.*, 2002] we suggested that satellite data that distinguish fine from coarse aerosols can be used for this purpose. The reason is that natural and anthropogenic aerosols have different proportions of fine and coarse aerosols. Urban/industrial pollution and smoke from vegetation burning (mostly anthropogenic) have mostly fine aerosol, while dust and marine aerosols (mostly natural) are dominated by coarse aerosol but with significant fine aerosol fraction [*Tanré et al.*, 2001; *Kaufman et al.*, 2001].

[4] Here we use MODIS measurements over the oceans of the aerosol optical thickness and the fraction of the optical thickness contributed by fine aerosol [*Tanré et al.*, 1997; *Remer et al.*, 2005], to derive the anthropogenic optical thickness. The results are used to evaluate chemical transport models that are used to assess the aerosol forcing of climate.

2. Analysis

[5] The method for satellite based estimate of the aerosol anthropogenic component is based on the following assumptions:

[6] 1) The fraction of the aerosol optical thickness contributed by the fine aerosol is constant for a given aerosol type; e.g. fine aerosol dominates the optical properties for smoke and pollution and coarse aerosol dominates dust and maritime aerosol.

[7] 2) All smoke is from anthropogenic origin and all dust is natural. It is estimated that about 20% of biomass burning originates from wild fires [*Hobbs et al.*, 1997]. About 10% of the dust can be from anthropogenic sources [*Tegen et al.*, 2004]. We shall account for the smoke overestimate but not dust later in the paper.

[8] 3) MODIS derivation of the fine fraction is consistent: any errors in the derivation of the fine fraction are constant and the correlation with the true fine fraction is very good.

[9] 4) Based on AERONET and MODIS analysis [*Kaufman et al.*, 2001, 2005] it is assumed that the baseline marine aerosol optical thickness is 0.06 ± 0.01. This is the average marine optical thickness for calm conditions. Strong winds can elevate the sea salt concentration.

[10] We represent the total aerosol optical thickness τ_{550} by its anthropogenic (air pollution and smoke aerosol) - τ_{anth}, dust - τ_{dust}, and baseline marine - τ_{mar}, components:

$$\tau_{550} = \tau_{anth} + \tau_{dust} + \tau_{mar} \qquad (1)$$

The fine aerosol optical thickness, τ_f, measured by the satellite can be described as:

$$\tau_f = f_{550}\tau_{550} = f_{anth}\tau_{anth} + f_{dust}\tau_{dust} + f_{mar}\tau_{mar} \qquad (2)$$

[1]NASA Goddard Space Flight Center, Greenbelt, Maryland, USA.
[2]Climate, Chemistry, and Ecosystems Team, Met Office, Exeter, UK.
[3]Formerly at Laboratoire d'Optique Atmospherique, CNRS, Université des Sciences et Technologies de Lille 1, Villeneuve d'Ascq, France.
[4]Laboratoire d'Optique Atmospherique, CNRS, Université des Sciences et Technologies de Lille 1, Villeneuve d'Ascq, France.
[5]Permanently at Research Institute for Applied Mechanics, Kyushu University, Fukuoka, Japan.

Dust transport and deposition observed from the Terra-Moderate Resolution Imaging Spectroradiometer (MODIS) spacecraft over the Atlantic Ocean

Y. J. Kaufman,[1] I. Koren,[2,3] L. A. Remer,[1] D. Tanré,[4] P. Ginoux,[5] and S. Fan[5]

[1]   Meteorological observations, in situ data, and satellite images of dust episodes were used already in the 1970s to estimate that 100 Tg of dust are transported from Africa over the Atlantic Ocean every year between June and August and are deposited in the Atlantic Ocean and the Americas. Desert dust is a main source of nutrients to oceanic biota and the Amazon forest, but it deteriorates air quality, as shown for Florida. Dust affects the Earth radiation budget, thus participating in climate change and feedback mechanisms. There is an urgent need for new tools for quantitative evaluation of the dust distribution, transport, and deposition. The Terra spacecraft, launched at the dawn of the last millennium, provides the first systematic well-calibrated multispectral measurements from the Moderate Resolution Imaging Spectroradiometer (MODIS) instrument for daily global analysis of aerosol. MODIS data are used here to distinguish dust from smoke and maritime aerosols and to evaluate the African dust column concentration, transport, and deposition. We found that 240 ± 80 Tg of dust are transported annually from Africa to the Atlantic Ocean, 140 ± 40 Tg are deposited in the Atlantic Ocean, 50 Tg fertilize the Amazon Basin (four times as previous estimates, thus explaining a paradox regarding the source of nutrition to the Amazon forest), 50 Tg reach the Caribbean, and 20 Tg return to Africa and Europe. The results are compared favorably with dust transport models for maximum particle diameter between 6 and 12 μm. This study is a first example of quantitative use of MODIS aerosol for a geophysical research.

1. Introduction

[2]   *Prospero and Carlson* [1972], *Prospero and Nees* [1977] and *Carlson* [1979] used meteorological observations, in situ data and satellite images (AVHRR) of dust episodes, to derive the first estimates of dust emission from Africa of 100 Tg of dust for a latitude belt 5°–25°N in the summer months June to August. This estimate was done before inaccuracies with AVHRR calibration were recognized and corrected [*Holben et al.*, 1990]. Owing to lack of systematic satellite measurements designed for aerosol studies, improvements in the estimates of dust emission were based mainly on models of the dust sources, emission and transport [*Tegen and Fung*, 1994; *Prospero et al.*, 1996;

Ginoux et al., 2001]. With the launch of the first Moderate Resolution Imaging Spectroradiometer (MODIS) instrument at the end of 1999, quantitative and systematic measurements of dust transport are possible [*Gao et al.*, 2001; *Kaufman et al.*, 2002] and presented here for the Atlantic ocean.

[3]   The constant flux of dust across the Atlantic Ocean is of considerable interest. In the last 10 years the citation index reports 500 papers about or related to Saharan dust, and shows an exponential increase in the publication rate, starting from the early works of Prospero and Carlson in the 1970s (see Figure 1). Iron contained in aeolian dust was shown to be an important micronutrient for ocean phytoplankton, which could contribute to fluctuation of CO_2 on climatic timescales [*Martin et al.*, 1991] and contribute to climate variations. *Erickson et al.* [2003] measured, using satellite data, the effect of dust deposition on ocean productivity. Over the millennia, dust was suggested to be the main fertilizer of the Amazon forest [*Swap et al.*, 1992]. Desert dust, now considered to originate mainly from natural source [*Tegen et al.*, 2004] interact with solar and thermal radiation, thus can modulate the Earth radiation balance in response to changing climate conditions [*Prospero et al.*, 2002], i.e., changes in

---

[1]NASA Goddard Space Flight Center, Greenbelt, Maryland, USA.
[2]National Research Council, Greenbelt, Maryland, USA.
[3]Now at NASA Goddard Space Flight Center, Greenbelt, Maryland, USA.
[4]Laboratoire d'Optique Atmospherique, CNRS, Université de Science et Technique de Lille, Villeneuve d'Ascq, France.
[5]NOAA Geophysical Fluids Dynamics Laboratory, Princeton University, Princeton, New Jersey, USA.

Comparison of Moderate Resolution Imaging Spectroradiometer (MODIS) and Aerosol Robotic Network (AERONET) remote-sensing retrievals of aerosol fine mode fraction over ocean

R. G. Kleidman,[1,2] N. T. O'Neill,[3] L. A. Remer,[4] Y. J. Kaufman,[4] T. F. Eck,[4,5] Didier Tanré,[6] Oleg Dubovik,[4] and B. N. Holben[4]

[1]   Aerosol particle size is one of the fundamental quantities needed to determine the role of aerosols in forcing climate, modifying the hydrological cycle, and affecting human health and to separate natural from man-made aerosol components. Aerosol size information can be retrieved from remote-sensing instruments including satellite sensors such as Moderate Resolution Imaging Spectroradiometer (MODIS) and ground-based radiometers such as Aerosol Robotic Network (AERONET). Both satellite and ground-based instruments measure the total column ambient aerosol characteristics. Aerosol size can be characterized by a variety of parameters. Here we compare remote-sensing retrievals of aerosol fine mode fraction over ocean. AERONET retrieves fine mode fraction using two methods: the Dubovik inversion of sky radiances and the O'Neill inversion of spectral Sun measurements. Relative to the Dubovik inversion of AERONET sky measurements, MODIS slightly overestimates fine fraction for dust-dominated aerosols and underestimates in smoke- and pollution-dominated aerosol conditions. Both MODIS and the Dubovik inversion overestimate fine fraction for dust aerosols by $0.1-0.2$ relative to the O'Neill method of inverting AERONET aerosol optical depth spectra. Differences between the two AERONET methods are principally the result of the different definitions of fine and coarse mode employed in their computational methodologies. These two methods should come into better agreement as a dynamic radius cutoff for fine and coarse mode is implemented for the Dubovik inversion. MODIS overestimation in dust-dominated aerosol conditions should decrease significantly with the inclusion of a nonspherical model.

Citation: Kleidman, R. G., N. T. O'Neill, L. A. Remer, Y. J. Kaufman, T. F. Eck, D. Tanré, O. Dubovik, and B. N. Holben (2005), Comparison of Moderate Resolution Imaging Spectroradiometer (MODIS) and Aerosol Robotic Network (AERONET) remote-sensing retrievals of aerosol fine mode fraction over ocean, *J. Geophys. Res.*, *110*, D22205, doi:10.1029/2005JD005760.

1.   Introduction

[2]   Aerosols play an important role in determining the Earth's radiation budget and in modifying clouds and precipitation [*Kaufman et al.*, 2002; *Rosenfeld and Lensky*, 1998]. Aerosols also adversely affect human health [*Samet et al.*, 2000]. Understanding the aerosols' physical and optical characteristics as well as their distribution patterns is necessary in order to forecast air quality and make

estimates of potential climate change [*Chu et al.*, 2003; *Kaufman et al.*, 2002].

[3]   One of the important physical characteristics of aerosols is their size. Knowing particle size distribution is critical to estimating the role of aerosols in Earth's energy balance, in determining the effect the particles will have on cloud development and on human health. In addition, aerosol size is the key to using satellite remote sensing to separate natural from man-made aerosols. Anthropogenic aerosol optical thickness is dominated by fine (mode) aerosol (effective radius between 0.1 and 0.25 μm), while natural aerosols contain a substantial component of coarse (mode) aerosol (effective radius between 1 and 2.5 μm) [*Kaufman et al.*, 2001; *Tanré et al.*, 2001]. Therefore measurement of the fine aerosol fraction or the ratio of fine to coarse mode can be used to identify and quantify the extent and role in climate of anthropogenic aerosol [*Kaufman et al.*, 2002].

[4]   Aerosol particle size parameters such as fraction of the fine mode or the ratio of fine to coarse mode can be measured by in situ volumetric and optical sampling mea-

[1]Science Systems and Applications, Inc., Greenbelt, Maryland, USA.
[2]Also at NASA Goddard Space Flight Center, Greenbelt, Maryland, USA.
[3]Centre d'Applications et de Recherches en Télédétection, Université de Sherbrooke, Sherbrooke, Quebec, Canada.
[4]NASA Goddard Space Flight Center, Greenbelt, Maryland, USA.
[5]Also at Goddard Earth Sciences and Technology Center, University of Maryland Baltimore County, Baltimore, Maryland, USA.
[6]Laboratoire d'Optique Atmosphérique, CNRS, Université des Sciences et Technologies de Lille, Villeneuve d'Ascq, France.

Aerosol invigoration and restructuring of Atlantic convective clouds

Ilan Koren,[1,2] Yoram J. Kaufman,[1] Daniel Rosenfeld,[3] Lorraine A. Remer,[1] and Yinon Rudich[4]

[1] Clouds and precipitation play crucial roles in the Earth's energy balance, global atmospheric circulation and the availability of fresh water. Aerosols may modify cloud properties and precipitation formation by modifying the concentration and size of cloud droplets, and consequently the strength of cloud convection, and height of glaciation levels thus affecting precipitation patterns. Here we evaluate the aerosol effect on clouds, using large statistics of daily satellite data over the North Atlantic Ocean. We found a strong correlation between the presence of aerosols and the structural properties of convective clouds. These correlations suggest systematic invigoration of convective clouds by pollution, desert dust and biomass burning aerosols. On average increase in the aerosol concentration from a baseline to the average values is associated with a 0.05 ± 0.01 increase in the cloud fraction and a 40 ± 5mb decrease in the cloud top pressure. **Citation:** Koren, I., Y. J. Kaufman, D. Rosenfeld, L. A. Remer, and Y. Rudich (2005), Aerosol invigoration and restructuring of Atlantic convective clouds, *Geophys. Res. Lett.*, *32*, L14828, doi:10.1029/2005GL023187.

1. Introduction

[2] Based on a few case studies, it has been suggested [*Andreae et al.*, 2004; *Williams et al.*, 2002] that the suppression of warm rain by aerosol causes most of the condensates to ascend, freeze and release the latent heat of freezing before precipitating. Delayed precipitation leads to more persistent updrafts and to more vigorous clouds before the precipitation-induced downdrafts take over. In addition, smaller droplets freeze at higher altitudes and at lower temperatures [*Rosenfeld and Woodley*, 2000]; therefore more latent heat is released higher in the atmosphere. The magnitude and robustness of these aerosol effects have not yet been investigated in a variety of meteorological conditions.

[3] Here we report strong correlations between aerosol loading and convective cloud properties. We see the correlations in all scales, from droplet scale to the extent and shape of the entire cloud. We show using large statistics that an increase in aerosol concentration correlates with changes in the cover, height and anvil portion of convective clouds.

We show these correlations occur repeatedly in three latitude belts of the Atlantic Ocean each with its own unique cloud dynamics and aerosol type.

2. Analysis

[4] We use three months (June-August 2002) of MODIS (MODerate resolution Imaging Spectroradiometer) [*Salomonson et al.*, 1989] Level 3 data from the Terra satellite over the northern Atlantic Ocean from 60°N to the Equator (covering ~4 billion km2). The satellite products include cloud fraction, optical thickness and droplet effective radius, each further partitioned by thermodynamic phase (ice/water), cloud top pressure and temperature [*King et al.*, 2003; *Platnick et al.*, 2003] and also by aerosol optical depth (AOD) at 550 nm [*Tanré et al.*, 1997; *Kaufman et al.*, 1997; *Remer et al.*, 2005]. MODIS measures daily cloud and aerosol reflection of sunlight with resolution of 0.25–1 km. The daily data are averaged into a 1-degree grid (MODIS algorithms, Level 3, available at http://modis-atmos.gsfc.nasa.gov/DAILY/atbd.html), that includes information on clouds and the surrounding aerosols (unless the grid box is completely overcast). We also used NCEP (National Center for Environmental Prediction) reanalysis [*Kalnay et al.*, 1996] and MODIS precipitable water vapor as a measure of the meteorology.

[5] In this study we focus on correlations between aerosols and the properties of deep convective and high cloud fields. Clouds were classified based on their top pressure, thermodynamic phase and cloud spatial homogeneity. Convective clouds are identified based on the variation in cloud top pressure among adjacent grid boxes and based on the optical depth of ice and water. The cloud classification algorithm was tuned on manually classified clouds followed by manual verification process of randomly selected cases. During the northern hemisphere summer, the average cloud fraction in the studied area is ~0.6, of which 75% are classified as deep convective and high clouds and 25% as marine stratocumulus and shallow cumulus (analyzed in a different study [*Kaufman et al.*, 2005]).

[6] We performed the analysis of the convective clouds separately for three regions characterized by different synoptic conditions: 0–15°N, including the ITCZ (Intertropical Convergence Zone), where the prevailing wind is easterly and carries mainly dust aerosol from the Sahara to the tropics of America; 16N–45N (sub tropical zone), where most of the deep convection develops in the southerlies along the Americas, transporting aerosols from the tropics to the mid-latitudes; and 46N–60N, where the system is dominated by the westerly wind that brings pollution aerosol from North America to Europe (mid-latitudes). In the tropical and mid-latitude zones the average flow is zonal (east-west) and the convective clouds are distributed

---

[1]NASA Goddard Space Flight Center, Greenbelt, Maryland, USA.
[2]JCET, University of Maryland, Baltimore County, Baltimore, Maryland, USA.
[3]Institute of Earth Sciences, Hebrew University of Jerusalem, Jerusalem, Israel.
[4]Department of Environmental Sciences, Weizmann Institute, Rehovot, Israel.

Cloud Inhomogeneity from MODIS

LAZAROS OREOPOULOS

JCET, University of Maryland, Baltimore County, Baltimore, and Laboratory for Atmospheres, NASA Goddard Space Flight Center, Greenbelt, Maryland

ROBERT F. CAHALAN

Laboratory for Atmospheres, NASA Goddard Space Flight Center, Greenbelt, Maryland

(Manuscript received 27 September 2004, in final form 16 June 2005)

ABSTRACT

Two full months (July 2003 and January 2004) of Moderate Resolution Imaging Spectroradiometer (MODIS) Atmosphere Level-3 data from the *Terra* and *Aqua* satellites are analyzed in order to characterize the horizontal variability of vertically integrated cloud optical thickness ("cloud inhomogeneity") at global scales. The monthly climatology of cloud inhomogeneity is expressed in terms of standard parameters, initially calculated for each day of the month at spatial scales of $1° \times 1°$ and subsequently averaged at monthly, zonal, and global scales. Geographical, diurnal, and seasonal changes of inhomogeneity parameters are examined separately for liquid and ice phases and separately over land and ocean. It is found that cloud inhomogeneity is overall weaker in summer than in winter. For liquid clouds, it is also consistently weaker for local morning than local afternoon and over land than ocean. Cloud inhomogeneity is comparable for liquid and ice clouds on a global scale, but with stronger spatial and temporal variations for the ice phase, and exhibits an average tendency to be weaker for near-overcast or overcast grid points of both phases. Depending on cloud phase, hemisphere, surface type, season, and time of day, hemispheric means of the inhomogeneity parameter ν (roughly the square of the ratio of optical thickness mean to standard deviation) have a wide range of $\sim$1.7 to 4, while for the inhomogeneity parameter χ (the ratio of the logarithmic to linear mean) the range is from $\sim$0.65 to 0.8. The results demonstrate that the MODIS Level-3 dataset is suitable for studying various aspects of cloud inhomogeneity and may prove invaluable for validating future cloud schemes in large-scale models capable of predicting subgrid variability.

1. Introduction

The nonlinear interplay of solar and longwave radiation with cloud optical properties is a fundamental aspect of atmospheric radiative transfer with implications for the earth's climate that were already noted many years ago (e.g., Harshvardhan and Randall 1985). In recent years, a plethora of studies examined various aspects of this interplay but, to our knowledge, only a handful was of global scope, namely the observational study of Rossow et al. (2002, hereafter RDC) and the model-based studies of Oreopoulos et al. (2004) and Räisänen et al. (2004). The present study, focusing only on a specific aspect of cloud variability, namely the horizontal fluctuations of total optical thickness τ

(hereafter "cloud inhomogeneity"), is also of global scope. Studies on this topic preceding RDC provided an incomplete and often conflicting picture of the magnitude of cloud inhomogeneity, as they were based on a limited number of scenes and different observational methods (Cahalan et al. 1994, 1995; Barker 1996; Oreopoulos and Davies 1998a; Pincus et al. 1999). In the following we make the case that, similar to the International Satellite Cloud Climatology Project (ISCCP) products used by RDC, higher-level cloud products from the Moderate Resolution Imaging Spectroradiometer (MODIS) instrument aboard the *Terra* and *Aqua* satellites can provide a detailed picture of cloud inhomogeneity.

Knowledge of the actual geographical and seasonal distribution of cloud inhomogeneity is essential in our effort to make it a diagnosed or predicted quantity that will improve representation of physical processes involving clouds in large-scale models (LSMs). These in-

Corresponding author address: Lazaros Oreopoulos, NASA Goddard Space Flight Center, Code 613.2, Greenbelt, MD 20771.
E-mail: lazaros@climate.gsfc.nasa.gov

The MODIS Aerosol Algorithm, Products, and Validation

L. A. REMER,* Y. J. KAUFMAN,* D. TANRÉ,[+] S. MATTOO,*,[&] D. A. CHU,[#],[**] J. V. MARTINS,*,[++]
R.-R. LI,[#],[##] C. ICHOKU,*,[&] R. C. LEVY,*,[&] R. G. KLEIDMAN,*,[&] T. F. ECK,[@],[@@] E. VERMOTE,[@],[&&]
AND B. N. HOLBEN[@]

*Laboratory for Atmospheres, NASA Goddard Space Flight Center, Greenbelt, Maryland
[+]Laboratoire d'Optique Atmospherique, Université des Sciences et Technologies de Lille, Villenueve d'Ascq, France
[#]Laboratory for Atmospheres, NASA Goddard Space Flight Center, Greenbelt, Maryland
[@]Laboratory for Terrestrial Physics, NASA Goddard Space Flight Center, Greenbelt, Maryland

ABSTRACT

The Moderate Resolution Imaging Spectroradiometer (MODIS) aboard both NASA's *Terra* and *Aqua* satellites is making near-global daily observations of the earth in a wide spectral range (0.41–15 μm). These measurements are used to derive spectral aerosol optical thickness and aerosol size parameters over both land and ocean. The aerosol products available over land include aerosol optical thickness at three visible wavelengths, a measure of the fraction of aerosol optical thickness attributed to the fine mode, and several derived parameters including reflected spectral solar flux at the top of the atmosphere. Over the ocean, the aerosol optical thickness is provided in seven wavelengths from 0.47 to 2.13 μm. In addition, quantitative aerosol size information includes effective radius of the aerosol and quantitative fraction of optical thickness attributed to the fine mode. Spectral irradiance contributed by the aerosol, mass concentration, and number of cloud condensation nuclei round out the list of available aerosol products over the ocean. The spectral optical thickness and effective radius of the aerosol over the ocean are validated by comparison with two years of Aerosol Robotic Network (AERONET) data gleaned from 132 AERONET stations. Eight thousand MODIS aerosol retrievals collocated with AERONET measurements confirm that one standard deviation of MODIS optical thickness retrievals fall within the predicted uncertainty of $\Delta\tau = \pm0.03 \pm0.05\tau$ over ocean and $\Delta\tau = \pm0.05 \pm 0.15\tau$ over land. Two hundred and seventy-one MODIS aerosol retrievals collocated with AERONET inversions at island and coastal sites suggest that one standard deviation of MODIS effective radius retrievals falls within $\Delta r_{\text{eff}} = \pm0.11$ μm. The accuracy of the MODIS retrievals suggests that the product can be used to help narrow the uncertainties associated with aerosol radiative forcing of global climate.

[&] Additional affiliation: Science Systems and Applications, Inc., Lanham, Maryland.

[**] Current affiliation: Joint Center for Earth Systems Technology, University of Maryland, Baltimore County, Baltimore, Maryland.

[++] Additional affiliation: Joint Center for Earth Systems Technology, University of Maryland, Baltimore County, Baltimore, Maryland.

[##] Current affiliation: Goddard Earth Sciences and Technology Center, University of Maryland, Baltimore County, Baltimore, Maryland.

[@@] Additional affiliation: Goddard Earth Sciences and Technology Center, University of Maryland, Baltimore County, Baltimore, Maryland.

[&&] Additional affiliation: Department of Geography, University of Maryland, College Park, College Park, Maryland.

Corresponding author address: Dr. Lorraine Remer, Code 913, NASA Goddard Space Flight Center, Greenbelt, MD 20771.
E-mail: Lorraine.A.Remer@nasa.gov

The influence of the several very large solar proton events in years 2000–2003 on the neutral middle atmosphere

Charles H. Jackman [a,*], Matthew T. DeLand [b], Gordon J. Labow [a,b],
Eric L. Fleming [a,b], Debra K. Weisenstein [c], Malcolm K.W. Ko [d],
Miriam Sinnhuber [e], John Anderson [f], James M. Russell [f]

[a] Code 916, Laboratory for Atmospheres, NASA Goddard Space Flight Center, Greenbelt, MD 20771, USA
[b] Science Systems and Applications, Inc., 10210 Greenbelt Road, Suite 400, Lanham, MD 20706, USA
[c] Atmospheric and Environmental Research, Inc., 131 Hartwell Avenue, Lexington, MA 02421, USA
[d] Mail Stop 401B, NASA Langley Research Center, Hampton, VA 23681, USA
[e] Institute of Environmental Physics, University of Bremen, Germany
[f] Hampton University, Center for Atmospheric Sciences, Hampton, VA 23668, USA

Abstract

Solar proton events (SPEs) are known to have caused changes in constituents in the Earth's polar neutral middle atmosphere. The past four years, 2000–2003, have been replete with SPEs. Huge fluxes of high energy protons entered the Earth's atmosphere in periods lasting 2–3 days in July and November 2000, September and November 2001 and October 2003. The highly energetic protons produce ionizations, excitations, dissociations and dissociative ionizations of the background constituents, which lead to the production of HO_x (H, OH, HO_2) and NO_y (N, NO, NO_2, NO_3, N_2O_5, HNO_3, HO_2NO_2, $ClONO_2$, $BrONO_2$). The HO_x increases lead to short-lived ozone decreases in the polar mesosphere and upper stratosphere due to the short lifetimes of the HO_x constituents. Large mesospheric ozone depletions (>70%) due to the HO_x enhancements were observed and modeled as a result of the very large July 2000 SPE. The NO_y increases lead to long-lived stratospheric ozone changes because of the long lifetime of the NO_y family in this region. Polar total ozone depletions >1% were simulated in both hemispheres for extended periods of time (several months) as a result of the NO_y enhancements due to the very large SPEs.
© 2004 COSPAR. Published by Elsevier Ltd. All rights reserved.

Keywords: Solar particle events; Odd nitrogen; Ozone; Middle atmosphere

1. Introduction

Explosions on the Sun sometimes result in large fluxes of high-energy solar protons at the Earth, especially near Solar Maximum. This period of time, wherein the solar proton flux is generally elevated for a few days, is known as a solar proton event (SPE). Solar cycle

* Corresponding author. Tel.: +1 301 614 6053; fax: +1 301 614 5903.
E-mail address: Charles.H.Jackman@nasa.gov (C.H. Jackman).

23 experienced a large number of extremely energetic SPEs in years 2000–2003. Huge fluxes of high-energy protons occurred in July and November 2000, September and November 2001 and October 2003.

Solar protons are guided by the Earth's magnetic field and impact both the northern and southern polar cap regions (>60° geomagnetic latitude), e.g., see Jackman and McPeters (2004). These protons can impact the neutral middle atmosphere (stratosphere and mesosphere) and produce ionizations, dissociative ionizations and excitations. Both HO_x (H, OH, HO_2) and NO_y (N, NO, NO_2,

Note on the effect of horizontal gradients for nadir-viewing microwave and infrared sounders

By J. JOINER[1]* and P. POLI[2,3]

[1]*NASA Goddard Space Flight Center, Laboratory for Atmospheres, Greenbelt, USA*
[2]*Joint Center for Earth Systems Technology, University of Maryland, Baltimore County, USA*
[3]*NASA Goddard Space Flight Center, Global Modeling and Assimilation Office, Greenbelt, USA*

SUMMARY

Passive microwave and infrared nadir sounders such as the Advanced Microwave Sounding Unit-A (AMSU-A) and the Atmospheric InfraRed Sounder (AIRS), both flying on NASA's EOS polar-orbiting Aqua satellite, provide information about vertical temperature and humidity structure that is used in data assimilation systems for numerical weather prediction and climate applications. These instruments scan across track so that, at the satellite swath edges, the satellite zenith angles can reach ~60°. The emission path through the atmosphere as observed by the satellite is therefore slanted with respect to the satellite footprint's zenith. Although radiative transfer codes currently in use at operational centres use the appropriate satellite zenith angle to compute brightness temperature, the input atmospheric fields are those from the vertical profile above the centre of the satellite footprint. If horizontal gradients are present in the atmospheric fields, the use of a vertical atmospheric profile may produce an error.

This note attempts to quantify the effects of horizontal gradients on AIRS and AMSU-A channels by computing brightness temperatures with accurate slanted atmospheric profiles. We use slanted temperature, water vapour, and ozone fields from data assimilation systems. We compare the calculated slanted and vertical brightness temperatures with AIRS and AMSU-A observations. We show that the effects of horizontal gradients on these sounders are generally small and below instrument noise. However, there are cases where the effects are greater than the instrument noise and may produce erroneous increments in an assimilation system. The majority of the affected channels have weighting functions that peak in the upper troposphere (water-vapour-sensitive channels) and above (temperature-sensitive channels) and are unlikely to significantly impact on tropospheric numerical weather prediction. However, the errors could be significant for other applications such as stratospheric analysis. Gradients in ozone and tropospheric temperature appear to be well captured by the analyses. In contrast, gradients in upper stratospheric and mesospheric temperature as well as upper-tropospheric humidity are less well captured. This is likely due in part to a lack of data to specify these fields accurately in the analyses. Advanced sounders, like AIRS, will help to better specify these fields in the future.

KEYWORDS: AIRS   AMSU   Assimilation   Azimuth angle   Radiances   Satellite

1. INTRODUCTION

The Atmospheric Infra-Red Sounder (AIRS) and the Advanced Microwave Sounding Unit-A (AMSU-A) (Aumann *et al.* 2003) are nadir-viewing passive sounders currently flying on the National Aeronautics and Space Administration's (NASA) Earth Observing System (EOS) polar-orbiting Aqua platform. AMSU-A also flies on the National Oceanic and Atmospheric Administration (NOAA) Polar Orbiting Environmental Satellites along with the High-resolution InfraRed Sounder (HIRS). These and other similar sounders are the primary satellite instruments used in atmospheric data assimilation systems (DASs) for numerical weather prediction and the production of climate datasets.

Fast radiative transfer models are used to compute brightness temperatures from background fields in a DAS. Analysis increments are then generated based on the difference between the observed and the computed brightness temperatures. The effects of so-called limb-brightening or limb-darkening across a scan line for an instrument on a polar-orbiting satellite are accounted for in the radiative transfer model by using an appropriate satellite zenith angle. However, the input atmospheric profile is usually the vertical one above the satellite footprint centre. The correct atmospheric profile should account for the fact that the emission path through the atmosphere is slanted with respect to the footprint zenith. If horizontal gradients are present, an error may occur if the vertical atmospheric path is used.

Horizontal gradient effects are a well-known problem for limb-viewing sounders. For example, gradient effects were shown to be important for the limb-viewing Global Positioning Satellite Radio Occultation sounding technique (e.g. Poli 2004; Poli and Joiner 2004).

* Corresponding author: NASA Goddard Space Flight Center, Code 916, Greenbelt, MD, 20771, USA.
e-mail: joanna.joiner@nasa.gov

**Atmospheric
Chemistry
and Physics**
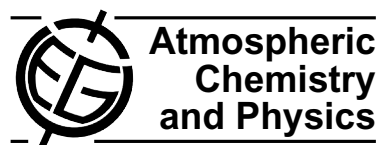
Fall vortex ozone as a predictor of springtime total ozone at high northern latitudes

S. R. Kawa[1], P. A. Newman[1], R. S. Stolarski[1], and R. M. Bevilacqua[2]

[1]Atmospheric Chemistry and Dynamics Branch, NASA Goddard Space Flight Center, Greenbelt, Maryland, USA
[2]Naval Research Laboratory, Washington, DC, USA

Abstract. Understanding the impact of atmospheric dynamical variability on observed changes in stratospheric O_3 is a key to understanding how O_3 will change with future climate dynamics and trace gas abundances. In this paper we examine the linkage between interannual variability in total column O_3 at northern high latitudes in March and lower-to-mid stratospheric vortex O_3 in the prior November. We find that these two quantities are significantly correlated in the years available from TOMS, SBUV, and POAM data (1978–2004). Additionally, we find that the increase in March O_3 variability from the 1980s to years post-1990 is also seen in the November vortex O_3, i.e., interannual variability in both quantities is much larger in the later years. The cause of this correlation is not clear, however. Interannual variations in March total O_3 are known to correspond closely with variations in winter stratospheric wave driving consistent with the effects of varying residual circulation, temperature, and chemical loss. Variation in November vortex O_3 may also depend on dynamical wave activity, but the dynamics in fall are less variable than in winter and spring. We do not find significant correlations of dynamic indicators for November such as temperature, heat flux, or polar average total O_3 with the November vortex O_3, nor with dynamical indicators later in winter and spring that might lead to a connection to March. We discuss several potential hypotheses for the observed correlation but do not find strong evidence for any considered mechanism. We present the observations as a phenomenon whose understanding may improve our ability to predict the dependence of O_3 on changing dynamics and chemistry.

1 Introduction

The polar regions are a bellwether for processes that affect stratospheric O_3 globally. Decadal decreases in total O_3 at high southern latitudes in spring (Fig. 1) are clearly attributable to increasing abundances of chlorine- and bromine-containing trace gases of anthropogenic origin, which are now regulated by international agreements (Solomon, 1999 and references within). Owing to more active meteorology in the northern hemisphere (NH), springtime O_3 decreases there are not as monotonic as those in the South (Fig. 1) and are attributed to a combination of chemical and dynamical forcings (Newman et al., 1997; Manney et al., 1997; Coy et al., 1997; Chipperfield and Jones, 1999; Anderson and Knudsen, 2002). The relative contribution, causal mechanisms, and time scales for dynamical O_3 change at high northern latitudes, as well as in the middle latitudes of both hemispheres, is currently the subject of active scientific debate (WMO, 2003).

During winter, O_3 is transported from the low-latitude photochemical production region by the poleward and downward Brewer-Dobson circulation. This circulation is primarily driven by planetary scale waves propagating into the stratosphere from the Northern extratropical troposphere (Rosenlof and Holton, 1993). These planetary waves affect polar O_3 is three ways: 1) directly, as noted above, by the Brewer-Dobson circulation which advects higher concentrations of O_3 into the lower stratosphere, 2) by occasionally mixing material into the polar vortex or by breaking up the polar vortex, and 3) indirectly by warming the polar region and reducing the occurrence of polar stratospheric clouds, which thereby decreases catalytic chemical loss of O_3. Interannual variation of planetary wave activity has a major effect on O_3 levels in spring via both transport and photochemical loss.

Correspondence to: S. R. Kawa
(kawa@maia.gsfc.nasa.gov)

Description and sensitivity analysis of a limb scattering ozone retrieval algorithm

R. P. Loughman,[1,2] D. E. Flittner,[1,3] B. M. Herman,[1] P. K. Bhartia,[4] E. Hilsenrath,[4] and R. D. McPeters[4]

[1]   We present the theoretical basis for an algorithm that retrieves vertical profiles of ozone concentration using measurements of light scattered from the limb of the atmosphere. Simulated radiances at wavelengths between 300 and 675 nm are inverted using the optimal estimation technique, producing a retrieved ozone number density profile between 10 and 55 km. A detailed sensitivity analysis of this ozone retrieval algorithm follows. The largest source of ozone retrieval error is tangent height misregistration (i.e., instrument pointing error), which is relevant throughout the altitude range of interest and produces retrieval errors on the order of $10-20\%$ due to a tangent height registration error of 0.5 km. The retrieved profile is shifted in altitude relative to the true profile, with very little distortion of the profile shape. Sensitivity to stratospheric aerosol is also a significant source of error, with errors of $5-8\%$ for altitudes less than 40 km under background aerosol conditions when an aerosol-free atmosphere is assumed by the algorithm. Using an incorrect a priori ozone estimate can produce errors up to 15% at altitudes near 10 km, but the a priori profile has little influence above that level. Addressing these error sources (e.g., with better instrument pointing knowledge, introduction of reliable aerosol information, and better instrument signal-to-noise to reduce the importance of the a priori ozone estimate, respectively) is the key to significantly improving the retrieval accuracy. Further improvement would then be limited by several secondary error sources that produce retrieval errors at the 5% level.

Citation: Loughman, R. P., D. E. Flittner, B. M. Herman, P. K. Bhartia, E. Hilsenrath, and R. D. McPeters (2005), Description and sensitivity analysis of a limb scattering ozone retrieval algorithm, *J. Geophys. Res.*, *110*, D19301, doi:10.1029/2004JD005429.

1.   Introduction

[2]   Measurements of scattered radiance in the limb of the atmosphere have been used to determine a variety of atmospheric properties, including stratospheric aerosol [*Cunnold et al.*, 1973; *Naudet and Thomas*, 1987; *McLinden et al.*, 1999], stratospheric temperature [*Rusch et al.*, 1983], mesospheric ozone concentration [*Rusch et al.*, 1984], upper-stratospheric NO_2 concentration [*Mount et al.*, 1984], and sensor attitude [*Janz et al.*, 1996; *Hilsenrath et al.*, 1997; *Sioris et al.*, 2001; *Kaiser et al.*, 2004]. The limb scatter (LS) technique has been proposed as a possible source of ozone profile information in the upper troposphere and lower stratosphere. These measurements can be made throughout the sunlit portion of the orbit, allowing global spatial coverage comparable to back-scattered ultraviolet (BUV) and thermal

emission (TE) methods. LS vertical resolution is inherently lower than (but comparable to) solar occultation (SO) vertical resolution, with $1-3$ km possible (depending on optical blurring), similar to TE resolution. Accurate ozone retrievals are possible throughout the stratosphere and possibly into the upper troposphere, again with performance similar to the SO and TE methods.

[3]   Several groups have developed new radiative transfer (RT) models to calculate the LS radiance [*Herman et al.*, 1995; *Oikarinen et al.*, 1999; *Griffioen and Oikarinen*, 2000; *Oikarinen*, 2001; *Kaiser*, 2001; *McLinden et al.*, 2002a, 2002b; *A. Rozanov et al.*, 2002; *V. Rozanov et al.*, 2002]. A brief description of the Gauss-Seidel Limb Scattering (GSLS) RT model used in this study can be found in Appendix A of *Loughman et al.* [2004]. The body of that paper describes an intercomparison study among several RT models, which established that the GSLS model agrees well with several other methods for a variety of LS measurement conditions. However, detailed sensitivity studies are required to predict the achievable performance of the LS ozone retrieval technique. The purpose of this paper is to present the theoretical basis for a LS ozone inversion algorithm, as well as describe its sensitivity to various perturbations, in greater detail than was possible in the work of *Flittner et al.* [2000]. It must be stressed that the retrieval procedure described herein is meant to be fairly simple and generic

---

[1]Institute of Atmospheric Physics, University of Arizona, Tucson, Arizona, USA.
[2]Now at Center for Atmospheric Sciences, Hampton University, Hampton, Virginia, USA.
[3]Now at Climate Science Branch, NASA Langley Research Center, Hampton, Virginia, USA.
[4]Laboratory for Atmospheres, Atmospheric Chemistry and Dynamics Branch, NASA Goddard Space Flight Center, Greenbelt, Maryland, USA.

Version 8 SBUV ozone profile trends compared with trends from a zonally averaged chemical model

Joan E. Rosenfield

Goddard Earth Science and Technology Center, University of Maryland Baltimore County, Baltimore, Maryland, USA

Stacey M. Frith

Science Systems and Applications Inc., Lanham, Maryland, USA

Richard S. Stolarski

Atmospheric Chemistry and Dynamics Branch, NASA Goddard Space Flight Center, Greenbelt, Maryland, USA

[1] A statistical time series analysis was applied to the new version 8 merged Solar Backscatter Ultraviolet (SBUV) data set of ozone profiles for the years 1979–2003. Linear trends for the 1979–1997 time period are reported and are compared to trends computed using ozone profiles from the Goddard Space Flight Center (GSFC) zonally averaged coupled model. Observed and modeled annual trends between 50°N and 50°S were a maximum in the higher latitudes of the upper stratosphere, with Southern Hemisphere (SH) trends greater than Northern Hemisphere (NH) trends. The observed upper stratospheric maximum annual trend is -7.0 ± 2.0%/decade (2σ) at 47.5°S and -4.7 ± 1.3%/decade at 47.5°N, to be compared with the modeled trends of -5.8 ± 0.3%/decade in the SH and -5.2 ± 0.3%/decade in the NH. Both observed and modeled trends are most negative in winter and least negative in summer, although the modeled seasonal difference is less than observed. Model trends are shown to be greatest in winter because of a repartitioning of chlorine species and the increasing abundance of chlorine with time. The model results illustrate the trend differences that can occur at 3 hPa depending on whether ozone profiles are in mixing ratio or number density coordinates and on whether they are recorded on pressure or altitude levels.

Citation: Rosenfield, J. E., S. M. Frith, and R. S. Stolarski (2005), Version 8 SBUV ozone profile trends compared with trends from a zonally averaged chemical model, *J. Geophys. Res.*, *110*, D12302, doi:10.1029/2004JD005466.

1. Introduction

[2] Stratospheric ozone profile measurements have been made by the Solar Backscatter Ultraviolet instruments (SBUV and SBUV/2) since November 1978. *Hood et al.* [1993] estimated ozone trends using Nimbus 7 SBUV data for the period November 1978 to June 1990. They found maximum upper stratospheric annual trends, poleward of 50°, of approximately -8%/decade in the Northern Hemisphere (NH) and approximately -12%/decade in the Southern Hemisphere (SH). Depletions increased with increasing latitude in both hemispheres. They reported maximum upper stratospheric high-latitude negative trends in the late fall and early winter seasons.

[3] *Hollandsworth et al.* [1995] combined reprocessed Nimbus 7 SBUV ozone data with observations from the SBUV/2 instrument on NOAA 11, and computed updated profile trends for the period November 1978 through June 1994. They found a general pattern of ozone loss similar to that computed by *Hood et al.* [1993], but obtained smaller

negative trends with the additional data. Maximum high-latitude upper stratospheric trends were approximately -8%/decade in the NH and approximately -10%/decade in the SH. They also reported maximum high-latitude upper stratospheric negative trends in the late fall and early winter.

[4] A large group of research scientists [*World Meteorological Organization (WMO)*, 1998; *Randel et al.*, 1999; *Newchurch et al.*, 2000; *Cunnold et al.*, 2000] reevaluated the vertical distribution of ozone trends for the period 1979 to 1996, including trends from the SBUV and the Stratospheric Gas and Aerosol Experiment (SAGE) instruments. They confirmed the previously reported latitudinal structure of trends, i.e., a maximum negative trend in the extra tropics and a minimum negative trend in the tropics, with a minimum downward trend at all latitudes at ~30 hPa. They concluded that SAGE trends were more negative than SBUV trends at nearly all latitudes. In the midlatitudes maximum upper stratospheric trends were approximately -9%/decade for SAGE and approximately -5%/decade for SBUV. SAGE annual trends were shown to have no statistically significant interhemispheric difference. They found that although SBUV upper stratospheric annual trends were more negative in the SH than the NH, this difference

Total Ozone Mapping Spectrometer measurements of aerosol absorption from space: Comparison to SAFARI 2000 ground-based observations

O. Torres,[1,2] P. K. Bhartia,[3] A. Sinyuk,[1,4] E. J. Welton,[3] and B. Holben[3]

[1]   The capability to detect the presence of absorbing aerosols in the atmosphere using space-based near-UV observations has been demonstrated in the last few years, as indicated by the widespread use by the atmospheric sciences community of the Total Ozone Mapping Spectrometer (TOMS) aerosol index as a qualitative representation of aerosol absorption. An inversion procedure has been developed to convert the unique spectral signature generated by the interaction of molecular scattering and particle absorption into a quantitative measure of aerosol absorption. In this work we evaluate the accuracy of the near-UV method of aerosol absorption sensing by means of a comparison of TOMS retrieved aerosol single scattering albedo and extinction optical depth to ground-based measurements of the same parameters by the Aerosol Robotic Network (AERONET) for a 2-month period during the SAFARI 2000 campaign. The availability of collocated AERONET observations of aerosol properties, as well as Micropulse Lidar Network measurements of the aerosol vertical distribution, offered a rare opportunity for the evaluation of the uncertainty associated with the height of the absorbing aerosol layer in the TOMS aerosol retrieval algorithm. Results of the comparative analysis indicate that in the absence of explicit information on the vertical distribution of the aerosols, the standard TOMS algorithm assumption yields, in most cases, reasonable agreement of aerosol optical depth (±30%) and single scattering albedo (±0.03) with the AERONET observations. When information on the aerosol vertical distribution is available, the accuracy of the retrieved parameters improves significantly in those cases when the actual aerosol profile is markedly different from the idealized algorithmic assumption.

1. Introduction

[2]   The role of atmospheric aerosols in the global climate is one of the largest remaining sources of uncertainty in the assessment of global climate change. Aerosols directly affect the energy balance of the Earth-atmosphere system, through the processes of scattering of solar radiation, which redistributes the incoming solar energy in the atmosphere, and absorption (of both solar and infrared radiation), which transforms radiative energy into internal energy of the absorbing particles and heats up the atmosphere. In addition, aerosols, through their role as cloud condensation nuclei, have an indirect effect on climate by affecting the albedo and lifetime of clouds [*Haywood and Boucher*, 2000].

[3]   The cooling effect of aerosols, associated with the backscattering to space of a fraction of the incoming solar energy, is considered to be a very important counteracting factor of the well known warming effect of the greenhouse gases. The absorption by aerosol particles of a fraction of the incident sunlight and, for certain aerosol types, infrared radiation, results in a heating of the atmosphere. Thus aerosol absorption reduces the cooling effect commonly associated with aerosol particles. Although, the impact of aerosol absorption on climate is still a subject of considerable debate [*Penner et al.*, 2003], recently published theoretical analysis suggest that black carbon may be the second most important global warming substance (in terms of its direct radiative forcing effect) after carbon dioxide, and larger than methane [*Jacobson*, 2002]. The role of aerosol absorption effects on climate is, therefore, an issue that needs to be better understood in order to reduce the currently large uncertainties of its climatic effect.

[4]   In this paper, we present and discuss the results of the application of the near-UV method to observations by

---

[1]Joint Center for Earth Systems Technology, University of Maryland, Baltimore County, Baltimore, Maryland, USA.

[2]Also at NASA Goddard Space Flight Center, Greenbelt, Maryland, USA.

[3]NASA Goddard Space Flight Center, Greenbelt, Maryland, USA.

[4]Now at Science Systems and Applications Inc., Lanham, Maryland, USA.

Operator representation as a new differential optical absorption spectroscopy formalism

Mark Wenig, Bernd Jähne, and Ulrich Platt

UV–visible absorption spectroscopy with extraterrestrial light sources is a widely used technique for the measurement of stratospheric and tropospheric trace gases. We focus on differential optical absorption spectroscopy (DOAS) and present an operator notation as a new formalism to describe the different processes in the atmosphere and the simplifying assumptions that compose the advantage of DOAS. This formalism provides tools to classify and reduce possible error sources of DOAS applications. © 2005 Optical Society of America

OCIS codes: 300.1030, 070.6020, 010.1290, 280.1120.

1. Introduction

A spectral signal on its way from generation in the light source through the atmosphere to the instrument experiences many different transformations. In this paper we introduce a formalism allowing a comparison of those transformations and the corresponding features of differential optical absorption spectroscopy (DOAS).[1] In this comparison we especially aim at the sequencing of the different transformations, each described by an operator, and identify some combination of noncommuting operators that can be assigned to effects such as the I_0 effect or the undersampling problem. Since these effects are based on different instrument and DOAS parameters, the classification of the main error sources can be helpful for the design of new DOAS instruments and to reduce the errors of existing DOAS applications.

2. Differential Optical Absorption Spectroscopy

In this section we describe the DOAS method. The absorption of radiation by matter is described by the Beer–Lambert law. The absorption of light of the intensity $I(\lambda)$ at the wavelength λ as it passes through an absorbing matter dl is

$$I(\lambda) = I_0(\lambda)\exp\left[-\sigma(\lambda,\ T)\int c(l)\mathrm{d}l\right]. \qquad (1)$$

Here $I_0(\lambda)$ is the incident light intensity, $I(\lambda)$ is the transmitted light intensity, $\sigma(\lambda, T)$ is the absorption cross section of the absorbing species that depends on the wavelength and temperature, and $c(l)$ is its concentration. Here the first simplifying assumption is made, namely, the temperature independence of the absorption cross sections. The cross sections can vary with altitude and temperature; therefore excluding it from the integration produces an error. We can reduce this error by using several cross sections for different temperatures, or, if those are linear dependent, by performing *a posteriori* temperature corrections for known temperature profiles. For most applications it is sufficient to use the temperature at the number density maximum of the climatological profile of the corresponding trace gas.[2]

When absorptions are measured in the atmosphere, Eq. (1) has to be applied for the absorption of all trace gases and has to deal with influences of scattering:

$$I(\lambda) = I_0(\lambda)\exp\left[-\sum_i \sigma_i(\lambda)\mathrm{SCD}_i\right]g(\lambda). \qquad (2)$$

where the factor $g(\lambda)$ describes additional attenuation by the optical system and by Rayleigh and Mie scattering in the atmosphere and all other broadband structured influences, such as reflection on the ground. The sum in the exponential runs over all

M. Wenig (wenig@gsfc.nasa.gov) is with NASA Goddard Space Flight Center, Greenbelt, Maryland 20771. B. Jähne and U. Platt are with the Institut für Umweltphysik, Heidelberg University, Heidelberg, Germany. B. Jähne is also with the Interdisciplinary Center for Scientific Computing, Heidelberg University, Heidelberg, Germany.